

A peer-reviewed version of this preprint was published in PeerJ on 2 April 2018.

[View the peer-reviewed version](https://peerj.com/articles/4579) (peerj.com/articles/4579), which is the preferred citable publication unless you specifically need to cite this preprint.

Castanera D, Belvedere M, Marty D, Paratte G, Lapaire-Cattin M, Lovis C, Meyer CA. 2018. A walk in the maze: variation in Late Jurassic tridactyl dinosaur tracks from the Swiss Jura Mountains (NW Switzerland) PeerJ 6:e4579 <https://doi.org/10.7717/peerj.4579>

A walk in the maze: Variation in Late Jurassic tridactyl dinosaur tracks - A case study from the Late Jurassic of the Swiss Jura Mountains (NW Switzerland)

Diego Castanera ^{Corresp., 1}, Matteo Belvedere ², Daniel Marty ², Géraldine Paratte ², Marielle Lapaire-Cattin ², Christel Lovis ², Christian A Meyer ³

¹ GeoBioCenter, Ludwig-Maximilians-Universität, Bayerische Staatssammlung für Paläontologie und Geologie, Munich, Germany

² Section d'archéologie et paléontologie, Paléontologie A16, Office de la culture,, Porrentruy, Switzerland

³ Department of Environmental Sciences, University of Basel, Basel, Switzerland

Corresponding Author: Diego Castanera
Email address: dcastanera@unizar.es

Background. Minute to medium-sized (FL less than 30 cm) tridactyl dinosaur tracks are the most abundant in the Late Jurassic tracksites of Highway A16 (Reuchenette Formation, Kimmeridgian) in the Jura Mountains (NW Switzerland). During excavations, two morphotypes, one gracile and one robust, were identified in the field. Furthermore, two large-sized theropod ichnospecies (*Megalosauripus transjuranicus* and *Jurabrontes curtedulensis*) and an ornithopod-like morphotype (Morphotype II) have recently been described at these sites. **Methods.** The quality of preservation (preservation grade), the depth of the footprint, the shape variation and the footprint proportions (FL/FW ratio and mesaxony) along the trackways have been analysed using 3D models and false-colour depth maps in order to determine the exact number of morphotypes present in the tracksites. **Results.** The study of the footprints (n = 93) collected during the excavations has made it possible to identify and characterize the two morphotypes distinguished in the field. The gracile morphotype is mainly characterized by a high footprint length/width ratio, high mesaxony, low divarication angles and clear, sharp claw marks and phalangeal pads (2-3-4). By contrast, the robust morphotype is characterized by a lower footprint length/width ratio, weaker mesaxony, slightly higher divarication angles and clear, sharp claw marks (when preserved), whereas the phalangeal pads are not clearly preserved although they might be present. **Discussion.** The analysis does not allow the two morphotypes to be associated within a morphological continuum. Thus, they cannot be a consequence of extramorphological variations on similar tracks produced by a similar/single trackmaker. Comparison of the two morphotypes with the larger morphotypes described in the formation (*Megalosauripus transjuranicus*, *Jurabrontes curtedulensis* and Morphotype II) and the spatio-temporal relationships of the trackways suggest that the smaller morphotypes cannot reliably be considered small individuals of

the larger morphotypes. The morphometric data of some specimens of the robust morphotype (even lower values for the length/width ratio and mesaxony) suggest that more than one ichnotaxon might be represented within the robust morphotype. The features of the gracile morphotype (cf. *Kalohipus*) are typical of “grallatorid” ichnotaxa with low mesaxony whereas those of the robust morphotype (cf. *Therangospodus* and ?*Therangospodus*) are reminiscent of *Therangospodus pandemicus*. This work sheds new light on combining an analysis of variations in footprint morphology through 3D models and false-colour depth maps, with the study of possible ontogenetic variations and the identification of small-sized tridactyl ichnotaxa for the description of new dinosaur tracks.

1 A walk in the maze: Variation in Late Jurassic tridactyl dinosaur tracks - A case study from the
2 Late Jurassic of the Swiss Jura Mountains (NW Switzerland)

3 Diego Castanera¹, Matteo Belvedere², Daniel Marty², Géraldine Paratte², Marielle Lapaire-
4 Cattin², Christel Lovis², Christian A. Meyer³

5 ¹Bayerische Staatssammlung für Paläontologie und Geologie and GeoBioCenter, Ludwig-
6 Maximilians-Universität Munich, Munich, Germany

7 ²Office de la culture, Section d'archéologie et paléontologie, Paléontologie A16, Porrentruy,
8 Switzerland.

9 ³Department of Environmental Sciences, University of Basel, Basel, Switzerland

10 Corresponding author: Diego Castanera

11 Email address: dcastanera@hotmail.es; d.castanera@lrz.uni-muenchen.de

12 ABSTRACT

13 **Background.** Minute to medium-sized (FL less than 30 cm) tridactyl dinosaur tracks are the most
14 abundant in the Late Jurassic tracksites of Highway A16 (Reuchenette Formation, Kimmeridgian)
15 in the Jura Mountains (NW Switzerland). During excavations, two morphotypes, one gracile and
16 one robust, were identified in the field. Furthermore, two large-sized theropod ichnospecies
17 (*Megalosauripus transjuranicus* and *Jurabrontes curtedulensis*) and an ornithopod-like
18 morphotype (Morphotype II) have recently been described at these sites.

19 **Methods.** The quality of preservation (preservation grade), the depth of the footprint, the shape
20 variation and the footprint proportions (FL/FW ratio and mesaxony) along the trackways have
21 been analysed using 3D models and false-colour depth maps in order to determine the exact
22 number of morphotypes present in the tracksites.

23 **Results.** The study of the footprints (n = 93) collected during the excavations has made it
24 possible to identify and characterize the two morphotypes distinguished in the field. The gracile
25 morphotype is mainly characterized by a high footprint length/width ratio, high mesaxony, low
26 divarication angles and clear, sharp claw marks and phalangeal pads (2-3-4). By contrast, the
27 robust morphotype is characterized by a lower footprint length/width ratio, weaker mesaxony,
28 slightly higher divarication angles and clear, sharp claw marks (when preserved), whereas the
29 phalangeal pads are not clearly preserved although they might be present.

30 **Discussion.** The analysis does not allow the two morphotypes to be associated within a
31 morphological continuum. Thus, they cannot be a consequence of extramorphological variations
32 on similar tracks produced by a similar/single trackmaker. Comparison of the two morphotypes
33 with the larger morphotypes described in the formation (*Megalosauripus transjuranicus*,
34 *Jurabrontes curtedulensis* and Morphotype II) and the spatio-temporal relationships of the
35 trackways suggest that the smaller morphotypes cannot reliably be considered small individuals
36 of the larger morphotypes. The morphometric data of some specimens of the robust morphotype
37 (even lower values for the length/width ratio and mesaxony) suggest that more than one
38 ichnotaxon might be represented within the robust morphotype. The features of the gracile
39 morphotype (cf. *Kalohipus*) are typical of “grallatorid” ichnotaxa with low mesaxony whereas
40 those of the robust morphotype (cf. *Therangospodus* and ?*Therangospodus*) are reminiscent of
41 *Therangospodus pandemicus*. This work sheds new light on combining an analysis of variations
42 in footprint morphology through 3D models and false-colour depth maps, with the study of
43 possible ontogenetic variations and the identification of small-sized tridactyl ichnotaxa for the
44 description of new dinosaur tracks.

45 **Keywords:** Dinosaur ichnology, Theropods, Kimmeridgian, Reuchenette Formation

46 INTRODUCTION

47 Since the first reported sauropod tracks were found in the Lommiswil quarry (late Kimmeridgian,
48 Canton Solothurn) in the Swiss Jura Mountains (Meyer, 1990), dinosaur track discoveries have
49 increased considerably, and to date more than 25 tracksites have been documented in the cantons
50 of Jura, Bern, Neuchâtel and Solothurn. Most of these tracksites belong to the Kimmeridgian
51 Reuchenette Formation, and some of them to the Tithonian Twannbach Formation (Meyer &
52 Thüning, 2003; Marty, 2008; Marty & Meyer, 2012; Marty et al., 2013). Between 2002 and 2011,
53 six large tracksites were systematically excavated and documented by Palaeontology A16 prior to
54 the construction of Highway A16. These tracksites covered a surface area of 18,500 m², and a
55 total of 59 ichnoassemblages comprising over 14,000 tracks including 254 sauropod and 411
56 bipedal tridactyl dinosaur trackways were documented. Therefore, the Jura carbonate platform
57 has today become a key area for Late Jurassic dinosaur palaeoichnology (Marty, 2008; Marty &
58 Meyer, 2012).

59 Among the tridactyl dinosaur tracks, recent papers have described giant theropod tracks
60 (*Jurabrontes curtedulensis*, Marty et al., 2017) and large theropod tracks (*Megalosauripus*
61 *transjuranicus*, Razzolini et al., 2017), but most of the tridactyl tracks by far are the still largely
62 undescribed minute, small and medium-sized tracks (footprint length < 30 cm). Marty (2008)
63 described minute and small tridactyl tracks from the Chevenez—Combe Ronde tracksite and
64 tentatively attributed some of these to *Carmelopodus*. Since then, however, many other tracksites
65 and ichnoassemblages with minute to medium-sized tridactyl tracks have been discovered,
66 including some very well-preserved tracks of different morphotypes and some very long
67 trackways (up to 100 m).

68 In Europe, apart from the Swiss and French (Mazin, Hantzpergue & Pouech, 2016) Jura
69 Mountains, the main Late Jurassic deposits that have yielded minute to medium-sized tridactyl
70 dinosaur tracks are located in the Lusitanian Basin in Portugal (Antunes & Mateus, 2003; Santos,
71 2008), the Asturian Basin in Spain (Lockley et al., 2008; Piñuela, 2015), the Aquitanian Basin in
72 France (Lange-Badré et al., 1996; Mazin et al., 1997; Moreau et al., 2017), the Lower Saxony
73 Basin in NW Germany (Kaefer & Lapparent, 1974; Diedrich, 2011; Lallensack et al., 2015), and
74 several units in the Holy Cross Mountains in Poland (Gierliński, Niedźwiedzki & Nowacki,
75 2009). The units that date to around the Jurassic-Cretaceous boundary (Tithonian–Berriasian) in
76 the Iberian Range in Spain (Santisteban et al., 2003; Castanera et al., 2013a; Alcalá et al., 2014;
77 Campos-Soto et al., 2017) should also be mentioned. It is noteworthy that there is no correspon-
78 ce between the high number of small to medium-sized tridactyl tracks (assigned to both theropods
79 and ornithomimids) described and the scarce number of ichnotaxa defined. Besides the tracks from
80 the Combe Ronde tracksite tentatively assigned to *Carmelopodus* by Marty (2008), the main
81 small to medium-sized tridactyl tracks identified have been from Spain (*Grallator* and
82 *Anomoepus*, from several sites in Asturias, Lockley et al., 2008; Piñuela, 2015; Castanera,
83 Piñuela & García-Ramos, 2016), France (*Carmelopodus*, Loulle tracksite, Mazin, Hantzpergue &
84 Pouech, 2016), Poland (*Wildeckia*, cf. *Jialingpus* and *Dineichnus*, different units in the Holy
85 Cross Mountains, Gierliński, Niedźwiedzki & Nowacki, 2009), Germany (*Grallator*, Bergkirchen
86 tracksite, Diedrich, 2011) and Portugal (*Dineichnus* and ?*Therangospodus*, Lockley et al., 1998a;

87 Lockley, Meyer & Moratalla, 2000). Other significant Late Jurassic areas with minute to
88 medium-sized tridactyl dinosaur tracks are found in the USA (Foster & Lockley, 2006), Morocco
89 (Belvedere, Mietto & Ishigaki, 2010), China (Xing, Harris & Gierliński, 2011; Xing et al., 2016),
90 Yemen (Schulp & Al-Wosabi, 2012) and Turkmenistan (Lockley, Meyer & Santos, 2000; Fanti et
91 al., 2013).

92 Several recent papers have examined the variability in track morphology along trackways
93 (Razzolini et al., 2014, 2017; Lallensack, van Heteren, & Wings, 2016), showing how
94 pronounced changes can occur along a given trackway. Thus, sometimes it can be very difficult
95 to determine the exact number of ichnotaxa and clearly distinguish between them, especially
96 when the tracks are morphologically similar. This should be borne in mind particularly when
97 studying the material from Highway A16, where large theropod tracks have shown notable
98 variations in shape along the same trackway, sometimes representing even two different
99 morphotypes (Razzolini et al., 2017). In the case of the minute to medium-sized tridactyl tracks,
100 two different morphotypes were identified at first glance during the documentation of the
101 tracksites, one gracile and one more robust. The aim of this paper is to describe the minute to
102 medium-sized tridactyl tracks collected in the Jura Mountains (NW Switzerland). In this
103 description, special emphasis is put on the analysis of track morphology through 3D models and
104 possible variations in footprint shape along trackways in order to discern whether or not the
105 different morphotypes are a consequence of preservational variations. In addition, other factors
106 such as possible ontogenetic variations in the larger ichnospecies described in the formation are
107 also taken into account. Finally, we discuss the ichnotaxonomy of the tracks together with some
108 palaeoecological implications.

109 GEOGRAPHICAL AND GEOLOGICAL SETTING

110 The studied material comes from six different tracksites from Highway A16 and nearby areas
111 (Fig. 1A): (1) Courtedoux—Bois de Sylleux (CTD—BSY), (2) Courtedoux—Tchâfouè (CTD—
112 TCH), (3) Courtedoux—Béchat Bovais (CTD—BEB), (4) Courtedoux—Sur Combe Ronde
113 (CTD—SCR), (5) Chevenez—Combe Ronde (CHE—CRO); and (6) Chevenez—La Combe (CHE—
114 CHV). For the sake of simplicity BSY, TCH, BEB, SCR, CRO and CHV are used in the
115 publication.

116 All the tracksites are located in the Ajoie district about 6-8 km to the west of Porrentruy (Canton
117 Jura, NW Switzerland) and on the path of Swiss federal highway A16 except the Chevenez—La
118 Combe tracksite, which is a quarry located near the village of Chevenez. The first five tracksites
119 were systematically excavated level-by-level by the Palaeontology A16 (PALA16) from 2002
120 until 2011 (Marty et al., 2003; Marty et al., 2004; Marty et al., 2007; Marty, 2008).

121 Geologically, the study area belongs to the Tabular Jura Mountains and is located at the eastern
122 end of the Rhine-Bresse transfer zone between the Folded Jura Mountains (South and East) and
123 the Upper Rhine Graben and Vosges Mountains (North). The Upper Jurassic strata of the Swiss
124 Jura Mountains are made up of shallow-marine carbonates deposited on the large and structurally

125 complex Jura carbonate platform, which was located at the northern margin of the Tethys at a
126 palaeolatitude of approximately 30° N (Thierry, 2000; Thierry et al., 2000; Stampfli & Borel,
127 2002).

128 The tracksites belong to the Kimmeridgian Reuchenette Formation, and the age is constrained by
129 the presence of ammonites to the *Cymodoce* to *Mutabilis* (Boreal), and *Divisum* to *Acanthicum*
130 (Tethyan) biozones (Comment et al., 2015). Accordingly, the age of the track-bearing levels is
131 late early to early late Kimmeridgian (Gygi, 2000; Comment et al., 2015). This age is also
132 confirmed by the presence of ostracods (Schudack et al., 2013). More information on the
133 sedimentology and palaeoenvironment of the Highway A16 tracksites can be found in Marty
134 (2008), Jank et al. (2006), Razzolini et al. (2017) and Marty et al. (2017).

135 Stratigraphically, the Highway A16 tracksites include three different track-bearing laminite
136 intervals, separated by shallow marine limestones (Marty, 2008; Waite et al., 2008; Comment,
137 Ayer & Becker, 2011; Comment et al., 2015). The three main track-bearing laminite intervals are
138 referred to as the lower, intermediate and upper levels, respectively levels 500–550, 1000–1100,
139 and 1500–1650 (Fig. 1B). Only tracks from the lower and intermediate track levels are included
140 in the present study (Fig. 1B), and the studied tracks come from a total of 11 different
141 ichnoassemblages (stratigraphic track levels). These are as follows: BEB500, CRO500,
142 BSY1020, BSY1040, BSY1050, TCH1055, SCR1055, TCH1060, TCH1065, TCH1069 and
143 CHV1000–1100 (precise level cannot be indicated).

144 MATERIAL AND METHODS

145 We analysed a total of 93 individual tracks (Table S1) that are housed in the track collection of
146 PALA16 (Canton Jura), either as original specimens or as replicas. The track collection will be
147 transferred to JURASSICA Muséum (Porrentruy, Canton Jura) in 2019. All the tracks are from
148 the aforementioned tracksites, the largest samples coming from BEB500 (39 footprints),
149 TCH1065 (15) and CRO500 (20). Each analysed track has two acronyms (Table S1): one
150 represents the number of the slab within the collection, e.g.: TCH006-1100 denotes Tchâfouè
151 tracksite, year 2006 (the year of discovery), slab 1100 (when the acronym has an “r” in front of
152 the specimen number, this means that it is a replica and not an original specimen). In the case of
153 the scanned footprints, these are referred to as “Laser-Scan”. A second acronym represents the
154 level and number of the trackway and track, e.g.: TCH1055-T2-L1 denotes Tchâfouè tracksite,
155 level 1055, trackway 2, track 1, left pes 1. The second acronym is used throughout the
156 manuscript. As the track-bearing layers were excavated level-by-level there are no doubts about
157 the preservation mode of the tracks. Thus, all the tracks were preserved as true tracks (concave
158 epireliefs) and were produced in the tracking surface, with the only exception of TCH1060-E58,
159 which was preserved as a natural cast (convex hyporelief).

160 . Preservation was described accordingly to the scale of Belvedere and Farlow (2016). Analysis
161 of track morphology was performed independently for each track; however, some tracks belong
162 to trackways and so were also analysed with a view to establishing the variation in footprint

163 morphology along a single trackway, thus trying to avoid over-identification of morphotypes.
164 These trackways are: BEB500-T16 (3), BEB500-T17 (4), BEB500-T58 (6), BEB500-T73 (4),
165 BEB500-T75 (2), BEB500-T78 (2), BEB-500-T82 (2), BEB-500-T93 (2), BEB500-T120 (4),
166 CRO500-T10 (14), CRO500-T30BIS (5), TCH1055-T2 (2), TCH1065-T15 (2), TCH1065-T25
167 (2) and TCH1069-T2 (2). We analysed each individual track and made an evaluation of the
168 quality of preservation according to the scale of Belvedere and Farlow (2016) (Table S1). As
169 stated by Belvedere and Farlow (2016), “quantitative shape analyses need to be based on data of
170 high quality, and comparisons are best made between tracks comparable in quality of
171 preservation”. Accordingly, only the tracks with a preservation grade equal to or higher than 2
172 were considered for measurement and analysis in this paper; field measurements exist for all the
173 other tracks and are stored in the PALA16 database. The descriptions are based on identification
174 of two different morphotypes, one gracile and one robust, during the documentation in the field.
175 Thus, the footprint length (FL), footprint width (FW), length and width of digits II (LII, WII), III
176 (LIII, WIII) and IV (LIV, WIV), divarication angles (II-III; III-IV) were measured (see Castanera,
177 Piñuela & García-Ramos, 2016, fig. 2). Subsequently, the FL/FW ratio and the mesaxony were
178 calculated. The latter was calculated on the basis of the anterior triangle length–width ratio (AT)
179 following Lockley (2009). All these measurements were taken from perpendicular pictures with
180 the software Image J. The tracks were classified according to different size classes (Marty, 2008)
181 on the basis of pes length (FL) as: 1) minute, FL < 10 cm; 2) small, 10 cm < FL < 20 cm; 3)
182 medium, 20 cm < FL < 30 cm; and 4) large, FL > 30 cm. The morphometric data of the studied
183 tracks were compared in a bivariate plot (length/width ratio vs. mesaxony) with larger tracks
184 (*Megalosauripus transjuranicus*, *Jurabrontes curtedulensis* and Morphotype II) described in the
185 Reuchenette Formation (Razzolini et al., 2017; Marty et al., 2017). In addition, they were also
186 compared with other theropod ichnotaxa using data from Castanera, Piñuela & García-Ramos
187 (2016) which were mainly compiled after Lockley (2009) and Xing et al. (2014). Data were
188 analysed with the software PAST v.2.14 (Hammer, Harper & Ryan, 2001). In addition, we
189 analysed the maximum depth of all the tracks, in order to ascertain whether there is a relationship
190 between this parameter, the preservation grade and the morphotype. The maximum depth was
191 estimated using the false-colour map derived from the 3D-model in those tracks with a
192 preservation grade generally higher than 0.5.

193 3D-photogrammetric models were generated from pictures taken with a Canon EOS 70D camera
194 equipped with a Canon 10-18mm STL lens using Agisoft Photoscan (v. 1.3.2, www.agisoft.com)
195 following the procedures of Mallison & Wings (2014) and Matthews, Noble & Breithaupt (2016).
196 Within the BEB500 sample, 3D data of 10 footprints were obtained by laser-scanning carried out
197 in the field in 2011 by Pöyry AG with a Faro hand-scanner, and most of these 10 footprints were
198 destroyed with the construction of Highway A16. The scaled meshes were exported as Stanford
199 PLY files (.ply) and then processed in CloudCompare (v.2.7.0, www.cloudcompare.com) in order
200 to obtain accurate false-colour depth maps. All photogrammetric meshes used in this study are
201 available for download here: <https://figshare.com/s/faf59ba7c717e99fd146> (ca. 2.5 Gb).

202 DESCRIPTION OF THE TRACK MORPHOTYPES:

203 Gracile morphotype:

204 This morphotype was identified in all six tracksites. The footprints are small to medium-sized
205 (15-21.2 cm) tridactyl tracks (Fig. 2), clearly longer than wide (FL/FW ratio = 1.50-1.90) (Table
206 1). The digits are slender with an acuminate end and clear claw marks preserved in the three
207 digits in the majority of the tracks. Digit III is clearly longer and slightly wider than digits II and
208 IV. Digits II and IV are similar in length and width. The mesaxony is variable but medium to high
209 (AT = 0.53-0.98), with a mean value of 0.77, although it is higher in most of the specimens (more
210 than 0.8 in half of the sample). The divarication angles are relatively low, II-III generally being
211 slightly higher (mean 25°) than III-IV (mean 22°). The hypices are quite symmetrical. The “heel”
212 morphology is variable; some specimens have an oval to round heel pad connected with digit IV
213 (BEB500-T16-R3, TCH1055-E53, TCH1055-T2-R1, TCH1069-T1-R2; see Fig.2), whereas in
214 others it is not clearly preserved even when the preservation grade is high (e.g.: BSY1020-E2).
215 Most of the specimens preserve a clear small medial notch located behind digit II, which with the
216 rounded heel marks gives them an asymmetric shape. Well-defined digital pads can be discerned
217 in some of the footprints. The tracks with the best quality of preservation suggest a phalangeal
218 formula of 2-3-4 (including the metatarsophalangeal pad IV).

219 Robust morphotype:

220 This morphotype has mainly been identified on the track levels BEB500 and TCH1065 (Fig. 3).
221 The footprints are small or medium-sized (17-21.8 cm) tridactyl tracks (Fig. 3), slightly longer
222 than wide (FL/FW ratio = 1.13-1.46), (Table 1). The digits are relatively robust with an
223 acuminate end and clear claw marks preserved in some of the tracks (e.g.: BEB500-T120-R5,
224 TCH1065-T15-R1, TCH1065-T21-R1). Digit III is clearly longer and slightly wider than digits II
225 and IV. Digits II and IV are similar in length and width. The mesaxony is variable but low-
226 medium (AT = 0.38-0.61), with a mean value of 0.49. The divarication angles are low, II-III
227 (mean 26°) and III-IV (mean 27°) being quite similar. The hypices are quite symmetrical. The
228 “heel” morphology is variable, ranging from subrounded to subtriangular. Only TCH1065-T21-
229 R1 preserves a clear small medial notch located behind digit II, thus being slightly asymmetrical,
230 whereas the other specimens are more symmetrical. Well-defined digital pads cannot be
231 discerned in most of the footprints, although TCH1065-T21-R1 shows digital pads suggesting a
232 possible phalangeal pad formula of 2-3-?4.

233 DESCRIPTION OF THE MORPHOLOGICAL VARIATIONS ALONG THE TRACKWAYS:

234 In this section we analyse the variations in footprint morphology (preservation grade and
235 maximum depth) along some of the trackways.

236 BEB500-T16:

237 It is a long turning trackway (Fig. 4A) of the gracile morphotype, composed of 27 footprints. It is
238 located in the northeastern part of the tracksite. Three consecutive footprints have been analysed.
239 The variation in preservation grade is high, even within a single step/stride, ranging from 2.5 in

240 BEB500-T16-R3 to 0.5 in BEB500-T16-R4. On the other hand, the variation in maximum depth
241 is only 1 cm between the three tracks (4.6 cm to 5.7 cm).

242 BEB500-T17

243 It is a very long, straight trackway (Fig. 4B) of the gracile morphotype, with 120 footprints
244 documented. The trackway crosses the whole surface of the site from the SE to the NW. Four
245 footprints were analysed. The preservation grade varies from 1 (BEB500-T17-L8) to 2 (BEB500-
246 T17-R8) while the maximum depth varies slightly less than 3 cm among the footprints (4.2 cm to
247 7 cm). It is interesting to note that the left tracks analysed (BEB500-T17-L8 and BEB500-T17-
248 L9) look more robust than the right ones (BEB500-T17-R8, BEB500-T17-R20), but on the other
249 hand are shallower.

250 BEB500-T58:

251 It is a long trackway (Fig. 4C) of the gracile morphotype, composed of 53 footprints. It is located
252 in the southeastern part of the tracksite and crosses through the middle of the site in a straight
253 southerly direction. It crosses trackways BEB500-T17, BEB500-T78 and BEB500-T82. Analysis
254 of six footprints suggests a variation in preservation grade from 0.5 (BEB500-T58-R22) to 1.5
255 (BEB500-T58-L22). The variation in maximum depth is around 2 cm (3.9 cm in BEB500-T58-
256 L22 to 6.2 cm BEB500-T58-L23).

257 BEB500-T73:

258 It is a short turning trackway (Fig. 4D) of the gracile morphotype, located in the northeastern part
259 of the site, and it runs in a NW/E direction. It crosses BEB500-T17 in the first part of the
260 trackway. Analysis of four tracks suggests a variation in preservation grade from 1 (BEB500-
261 T73-R4) to 2 (BEB500-T73-L5) and a variation in maximum depth of 2 cm (4.9 cm in BEB500-
262 T73-R5 to 6.9 cm in BEB500-T73-L5).

263 BEB500-T75:

264 It is a very long trackway (Fig. 4E) of the robust morphotype, with 71 footprints documented. It
265 is located in the southeastern part of the site, and crosses half of the site in a northerly direction.
266 Analysis of BEB500-T75-R12 and BEB-500-T75-R15 suggests a preservation grade of 1.5 and a
267 maximum depth of 3.3 cm in both tracks.

268 BEB500-T78:

269 It is a long trackway (Fig. 4F) of the gracile morphotype, composed of 24 footprints. It is located
270 in the northeastern part of the site. It crosses through the middle of the site in a straight W-E
271 direction. It crosses BEB500-T17 and BEB500-T82. Two footprints were analysed and the
272 preservation grade is 1 in both of them. The variation in maximum depth is very low (5.7 cm in
273 BEB500-T78-L5 and 6.2 cm in BEB500-T78-R3).

274 BEB500-T82:

275 It is a very long trackway (Fig. 4G) of the gracile morphotype, with 59 footprints documented. It
276 is located in the northeastern part of the site, crossing trackway BEB500-T78 to which it is
277 slightly subparallel. It also crosses BEB500-T17. It crosses almost the entire site running in a
278 straight W-E direction. Analysis of BEB-500-T82-R9 and BEB-500-T82-R14 revealed a
279 preservation grade of 1.5 and a variation in maximum depth of almost 2 cm (4.8 cm and 6.7 cm
280 respectively).

281 BEB500-T93:

282 It is a very long trackway (Fig. 4I) of the gracile morphotype, with 64 footprints preserved. It is
283 located in the northeastern part of the site and crosses the entire surface of the site in a straight W-
284 E direction. Analysis of BEB-500-T93-L5 and BEB-500-T93-R6 suggests a preservation grade of
285 1 and a variation in maximum depth of less than 0.5 cm (5.7 cm and 6.1 cm respectively).

286 BEB500-T120:

287 It is a long trackway (Fig. 4H) of the robust morphotype, composed of 29 footprints. It is located
288 in the southwestern part of the site and crosses half of the site in an almost straight W-E direction.
289 Four tracks were analysed, the preservation grade varying from 0 (BEB500-T120-L6) to 2
290 (BEB500-T120-R5, BEB500-T120-R6). The variation in maximum depth is one of the highest, at
291 almost 6 cm (4.2 cm in BEB500-T120-L5 to 10 cm in BEB500-T120-R6).

292 CRO500-T10:

293 It is a very long trackway (Fig. 5A) of the gracile morphotype (*Carmelopodus sensu* Marty,
294 2008), with 75 footprints documented. It crosses almost the entire surface of the site in a straight
295 SW-NE direction, making a small turning to the north in the last part of the trackway. Analysis of
296 14 footprints suggests a high variation in the preservation grade of the footprints, ranging
297 between 0 and 2 (CRO500-T10-L10). The variation in maximum depth is about 2 cm, ranging
298 from 3.1 cm (CRO500-T10-R3) to 5.7 cm (CRO500-T10-L5).

299 CRO500-T30BIS:

300 It is a short trackway (Fig. 5B) of the gracile morphotype, composed of 11 footprints. It is located
301 in the northeastern part of the site and crosses half of the site in an E-W direction. Analysis of
302 five footprints also suggests a high variation in the preservation grade of the footprints, ranging
303 between 0 (CRO500-T30BIS-L4) and 2 (CRO500-T30BIS-L5), even within a single stride. The
304 variation in maximum depth is 4.7 cm (from 5.3 cm in CRO500-T30BIS-L5 to 10 cm in
305 CRO500-T30BIS-R5), and is thus one of the highest. It is noteworthy that CRO500-T30BIS-R4
306 looks rather robust in comparison with the other tracks in the trackway, although this is not
307 related with the maximum depth, as CRO500-T30BIS-R5 is the one with a maximum depth of 10
308 cm.

309 TCH1055-T2:

310 It is a short trackway (Fig. 5C) of the gracile morphotype, composed of four footprints and
311 located in the northern part of the site. The trackway runs to the NW. Analysis of TCH1055-T2-
312 L1 and TCH1055-T2-R1 suggests a high preservation grade of 2-2.5 and a maximum depth of 5.1
313 cm and 7.6 cm, respectively.

314 TCH1065-T15:

315 It is a very short trackway (Fig. 5D) of the robust morphotype, with just two footprints
316 documented. It is located in the northern part of the site, and the trackway runs to the NW.
317 Analysis of TCH1065-T15-L1 and TCH1065-T15-R1 suggests a high variation in preservation
318 grade from 0.5 to 2, and a variation in maximum depth of 1.5 cm (6.8 cm and 8.3 cm
319 respectively).

320 TCH1065-T25:

321 It is a short trackway (Fig. 5F) of the gracile morphotype, composed of four footprints. It is
322 located in the northern part of the site, and the direction of the trackway is NW. Analysis of
323 TCH1065-T25-L2 and TCH1065-T25-R2 shows a preservation grade of 2 and 1, respectively,
324 and a high maximum depth of 10.2 cm and 12.9 cm, but not much variation (2.7 cm).

325 TCH1069-T2:

326 It is a short trackway (Fig. 5E) of the robust morphotype, with five footprints documented. It is
327 located in the northern part of the site, and the direction of the trackway is NE. Analysis of
328 TCH1069-T2-L2 and TCH1069-T2-R3 shows a preservation grade of 1 and 1.5 and a maximum
329 depth of 9.6 cm and 7.8 cm, respectively.

330 DISCUSSION:

331 1) True ichnodiversity or variation due to substrate-foot interaction?

332 The final shape of a footprint is determined by a combination of factors related to the anatomy of
333 the trackmaker's autopodium, the kinematics and the substrate (Marty et al., 2009; Falkingham,
334 2014); another important factor is the level in which the tracks were preserved (Milán &
335 Bromley, 2006), i.e. if they are preserved as undertracks. In the case of the tracksites of Highway
336 A16, we can rule out this factor as the excavation was carried out level-by-level, so the footprints
337 are true tracks (or natural casts). As the foot-substrate interaction is a major determinant of the
338 final shape of a track, it is important to analyse variations in depth and shape along trackways to
339 ascertain the morphological variation (e.g.: Razzolini et al., 2014). For this reason, we first
340 analysed the individual footprint shape (Figs. 2, 3) and then looked at the variation along the
341 trackway (Figs. 4, 5). The idea was to establish whether some of the described morphotypes
342 represent variations produced by the same/similar trackmakers walking in a substrate with
343 different properties (water content, thickness or cohesiveness). Previous researchers have
344 described variations between two extremes of a morphological continuum or a gradational series

345 (Gatesy et al., 1999; Razzolini et al., 2014) to suggest that similar theropods traversed substrates
346 of variable consistency. Only in such cases are the differences a consequence of foot-substrate
347 interactions rather than anatomical differences in the foot morphology of the trackmaker. In the
348 Swiss samples, clear evidence of intermediate morphologies is missing, supporting the presence
349 of at least two different groups of tridactyl trackmakers. Where gradational series of theropod
350 tracks have been reported (see refs above), these show a hallux, metatarsal marks, and distinctive
351 displacement rims in the deepest tracks that are clearly extramorphological features. None of the
352 morphotypes presented in this paper shows such evidence, even in the deepest tracks. This leads
353 us to think that the sediment was relatively firm during the production of the tracks.

354 Generally, tracks with a preservation grade of 1 or more can be classified in one of the two
355 described morphotypes: gracile or robust. There are just a few classification doubts regarding
356 isolated footprints (e.g.: CRO500-T30BIS-R4). At the outset, one possible hypothesis was that
357 the robust morphotype could be a variation on the gracile morphotype, produced by a similar
358 trackmaker on a substrate with different rheological properties (e.g.: Gatesy et al., 1999;
359 Razzolini et al., 2014, 2017). This hypothesis was especially appealing given the similar footprint
360 dimensions of the two morphotypes. Thus, the reasoning would be that the deeper tracks would
361 look more robust than the shallow ones, and the absence of clear phalangeal pad marks in most of
362 the robust morphotype tracks might be a consequence of a softer substrate or of deeper
363 penetration by the trackmaker foot. Indeed, according to our analysis of the maximum depth of
364 the footprints, those classified as belonging to the robust morphotype show some of the higher
365 values (e.g.: BEB500-T120-R5 = 6.1 cm; BEB500-T120-R6 = 10 cm; BEB500-E1 = 10.5 cm;
366 TCH1065-E124 = 6.9 cm; TCH1065-E188 = 5.9 cm; TCH1065-T15-R1 = 8.3 cm; TCH1065-
367 T21-R1 = 12.1 cm, see Table S1). Nonetheless, it is significant that the higher depth values for
368 the robust morphotype occur in level TCH1065, where also the gracile tracks show their deeper
369 values (TCH1065-E28 = 11.7 cm; TCH1065-T25-R2 = 12.9 cm; TCH1065-T25-L2 = 10.2 cm).
370 Therefore, on this track level the presence of the two morphotypes cannot be associated with the
371 depth of the footprints. In the case of BEB500 we see a similar scenario. In other words, some
372 tracks/trackways from the same level (e.g.: BEB500-T16 and BEB500-T17/ BEB500-T120 and
373 BEB500-E1) have similar depths, yet represent the gracile and robust morphotype, respectively.

374 The analysis of the morphological variation along the trackways shows that the gracile
375 morphotype is quite consistent along the trackways, and no tracks classifiable as robust are found
376 within these trackways. There are only a few cases, e.g. CRO500-T30BIS-R4 (Fig. 5B) and
377 BEB500-T17-L8/ BEB500-T17-L9 (Fig. 4B), which might look more robust than the other tracks
378 in the trackway, but here the features did not properly fit with the description of the robust
379 morphotype. Regarding the robust morphotype, in the analysed trackways (BEB500-T120,
380 TCH1065-T15 and TCH1069-T2) none of the tracks shows any feature of the gracile morphotype
381 (noteworthy is the low preservation grade and the scarce data for TCH1065-T15 and TCH1069-
382 T2). This suggests that, in our case, there is no clear correlation between the depth of the
383 footprint and the morphotypes and that the intra-trackway variation is never significant enough to
384 denote a shift between the morphotypes. Therefore, the present evidence indicates that there are

385 *at least* (see following discussion) two different trackmakers of minute to small-sized theropods
386 in the tidal flats of the Jura Mountains.

387 Analysis of the mesaxony and the FL/FW ratio supports the presence of *at least* the two
388 morphotypes (Fig. 6). Some authors have used mesaxony (Weems, 1992; Lockley, 2009) as a
389 good parameter to distinguish between tridactyl tracks. This parameter represents how far the
390 projection of digit III extends with respect to digits II and IV. In the studied sample, this
391 parameter is clearly lower in the robust morphotype than in the gracile one. The FL/FW ratio also
392 shows a considerable difference between the morphotypes (likewise lower in the robust
393 morphotype). A closer look at these two parameters within the robust morphotype (Fig. 6B) raises
394 the question whether it represents a single ichnotaxon. The data for the two analysed tracks from
395 BEB500-T120 show considerably lower data for the FL/FW ratio and weaker mesaxony than the
396 tracks from TCH1065 (see also following discussion).

397 2) Morphotype variation due to ontogeny?

398 Another salient point relating to the number of morphotypes in the analysed sample is the
399 possibility of variations due to different ontogenetic states. Few works have dealt with the
400 relationship between dinosaur footprints and ontogeny (e.g.: Lockley, 1994; Matsukawa, Lockley
401 & Hunt, 1999; Hornung et al., 2016). Ontogenetic variations have been suggested to explain
402 morphological variation in the classical theropod ichnotaxa of the *Grallator-Eubrontes* plexus
403 (Olsen, 1980; Olsen, Smith & McDonald, 1998; Moreau et al., 2012). Olsen, Smith & McDonald,
404 (1998) proposed that the major proportional differences between *Grallator*, *Anchisauripus* and
405 *Eubrontes* might be derived from the allometric growth of individuals of several related species.
406 In these typical theropod tracks the large tracks (*Eubrontes*) are wider with weaker mesaxony
407 than the smaller tracks (*Grallator*), showing a positive correlation between the elongation of the
408 track and the elongation of the anterior triangle (Lockley, 2009). As this author suggested, the
409 assumption of ontogenetic variation is thus based mainly on the assumption of a discernible
410 allometric pattern. Nonetheless, little is known about how possible ontogenetic variations may
411 have affected variations in footprint shape, and generally tracks that are similar in morphology
412 but different in size are considered to belong to the same ichnotaxon (Thulborn, 1990; Lockley,
413 1994; Matsukawa, Lockley & Hunt, 1999; Clark, Ross & Booth, 2005; Pascual-Arribas &
414 Hernández-Medrano, 2011). Demathieu (1990) also explored the use of ratios of length
415 characters to reduce the influence of size when comparing footprints. For instance, Lockley,
416 Mitchel & Odier (2007) assumed that small theropod tracks (*Carmelopodus*) from the Jurassic of
417 North America represent adults of small species and not juveniles of larger species and suggested
418 that “this inference is consistent with a model of rapid growth rates such as is typical of birds,
419 which would have reduced the number of potential track making juveniles that could habitually
420 make footprints”. By contrast, Pascual Arribas and Hernández-Medrano (2011) considered
421 minute theropod tracks from the Lower Cretaceous of Spain (subsequently assigned to *Kalohipus*
422 *bretunensis* by Castanera et al., 2015) to belong to baby theropods because of the morphometric
423 similarities with larger tracks from the same site and formation.

424 Different ontogenetic stages should also be considered in the interpretation of the Ajoie
425 ichnofauna. In one case, there are the similarities between the gracile morphotype and the
426 previously described *Carmelopodus* tracks from the Chevenez-Combe Ronde tracksite (CRO500-
427 T8; CRO500-T10; CRO500-T16; CRO500-T21; CRO500-T26; CRO500-T41). According to the
428 original description by Marty (2008), these tracks can be characterized as mesaxonic, slightly
429 asymmetric, tridactyl tracks that are clearly longer than wide. Digit III is always the longest, digit
430 IV being longer than digit II, which is shorter posteriorly. Claw impressions are present in the
431 three digits, and there is a phalangeal pad formula of 2-3-3. There is a low total divarication
432 angle, and divarication angles of the same order between digits II and III, and III and IV. It has a
433 narrow-gauge trackway with small tracks with outward rotation. CRO500-T10-L10 is the track
434 with the highest preservation grade recovered from level CRO500. Regarding the data taken from
435 this footprint, it should be noted that the FL/FW ratio (1.69) falls within the range of the other
436 gracile tracks, while the mesaxony is among the highest in the whole sample (0.96) but still
437 within the range of the gracile morphotype (Fig. 6). The divarication angle is also low (32°-23°).
438 Moreover, reanalysis of the tracks with the use of false-colour depth maps (Fig. 2F) allowed the
439 fourth phalangeal pad in digit IV to be distinguished, suggesting a formula of 2-3-4, although this
440 is not preserved in most of the tracks with a lower preservation grade (Fig. 5A). Accordingly, we
441 consider that there are not enough data to interpret these tracks as a different morphotype and we
442 regard them as part of the gracile morphotype. This result highlights the importance of analysing
443 large samples and the variation in shape through the trackways.

444 A second hypothesis considers whether the gracile and the robust morphotype might be
445 ontogenetic variations on the previously described larger ichnospecies (*Megalosauripus*
446 *transjuranicus* and *Jurabrontes curtedulensis*) of the Jura Mountains (Razzolini et al., 2017;
447 Marty et al., 2017). In fact, the two described ichnospecies represent large and more gracile
448 (*Megalosauripus transjuranicus*) and giant and more robust (*Jurabrontes curtedulensis*) theropod
449 tracks, respectively. In addition, a third large morphotype not assigned to any ichnotaxon and
450 named Morphotype II has also been described (Razzolini et al., 2017). This morphotype is
451 characterized by subsymmetric tracks that are generally slightly longer than wide (sometimes
452 almost as wide as long), blunt digit impressions, with no evidence for discrete phalangeal pad and
453 claw marks. These general features of the Morphotype II tracks are problematic because
454 sometimes trackways assigned to *Megalosauripus* also show these features when tracks are
455 poorly preserved. Thus, sometimes an extramorphological variation on *Megalosauripus* tracks
456 could be assigned to Morphotype II. There are also some tracks that constantly exhibit these
457 features through long trackways and that have been considered a third large unnamed ichnotaxon
458 with probable ornithopod affinities. These long trackways are found in the very surfaces that
459 many in the studied sample come from, such as BEB500 and CRO500 (Razzolini et al., 2017).
460 Thus, the hypothesis that the gracile and the robust morphotypes might represent
461 juvenile/subadult specimens of the larger tracks described in the tracksites must be explored.

462 Analysing footprint proportions, it should be noted that the FL/FW ratio of the gracile
463 morphotype fits within the upper range of the tracks included in *Megalosauripus* (Fig. 6A) from
464 the Reuchenette Formation; considering just the type material of *Megalosauripus transjuranicus*,

465 it fits completely (Fig. 6B) (Razzolini et al., 2017). On the other hand, the mesaxony is
466 substantially higher in the gracile morphotype than in the *Megalosauripus* tracks. In the case of
467 the robust morphotype, the FL/FW ratio fits within the range of the *Jurabrontes curtedulensis*
468 and Morphotype II tracks when analysing all the referred material (Fig. 6A) or just the type
469 material of *Jurabrontes curtedulensis* and the best-preserved tracks of Morphotype II (BEB500-
470 TR7-L2; BEB500-TR7-R2; BEB500-TR7-R7; BEB500-TR7-L10, Razzolini et al., 2017) (Fig.
471 6B). The robust morphotype has higher mesaxony than *Jurabrontes curtedulensis*, being more
472 similar in this respect to the Morphotype II tracks. It is notable that the footprint proportions
473 within the robust morphotype are quite variable between stratigraphic levels. For example, tracks
474 from trackway BEB500-T120 have a lower FL/FW ratio and mesaxony, whereas tracks from
475 track level TCH1065 have higher ratios. Thus, BEB500-T120 is closer to the ranges of
476 *Jurabrontes curtedulensis* whereas the tracks from TCH1065 are closer to the ranges of
477 *Megalosauripus transjuranicus* and especially the Morphotype II tracks (Fig. 6).

478 As we have discussed previously, the variations in mesaxony where larger tracks have lower
479 mesaxony are well documented in theropod tracks (Weems, 1992; Olsen, Smith & McDonald,
480 1998; Lockley, 2009). Because there are some overlapping areas in the footprint proportions of
481 the larger and the smaller tracks, it might be tempting to relate them according to these values;
482 i.e. gracile with *M. transjuranicus*, robust from BEB500 with *Jurabrontes*, and robust from
483 TCH1065 with Morphotype II. Nonetheless, the smaller morphotypes show other considerable
484 morphological differences apart from size and mesaxony with respect to the larger morphotypes.
485 The gracile morphotype differs from *M. transjuranicus* in key features of the diagnosis such as
486 the sigmoidal impression of digit III (less sigmoidal), the divarication angle (less divaricated) and
487 the digital pad of digit IV (proportionally smaller when preserved). The robust morphotype (from
488 both BEB500 and TCH1065) differs from *Jurabrontes curtedulensis* in the absence of clear
489 phalangeal pads (preservation bias?), the absence of the peculiar, isolated proximal pad PIII1 of
490 digit III, and the interdigital divarication angles (asymmetric vs symmetric); it differs from the
491 Morphotype II tracks in the absence of blunt digit impressions, possible evidence of a discrete
492 phalangeal pad, and the presence of clear claw marks.

493 Finally, we examine whether there is any spatiotemporal relationship between the larger and the
494 smaller tracks from the Ajoie ichnoassemblages. Lockley (1994) warned that the track data “that
495 most probably represent monospecific assemblages are those obtained for a single ichnotaxon
496 from a single bedding plane”. In this regard, it is interesting to note the scarcity of large theropod
497 tracks in the ichnoassemblages where both the gracile and the robust morphotype have been
498 identified, mainly levels BEB500, TCH1065 and CRO500. Level BEB500 (Fig. S2), the one with
499 the highest number of studied tracks ($n = 39$), is mainly composed of sauropods ($n = 17$
500 trackways) and minute to small tridactyl ($n = 158$ trackways) tracks. No tracks assigned to
501 *Jurabrontes curtedulensis* or *M. transjuranicus* have been documented in this level although it is
502 the surface with the most Morphotype II tracks ($n = 8$ trackways) documented. Level TCH1065
503 (Fig. S3) ($n = 15$ studied tracks) is composed of 189 tracks, mainly of minute to small-sized
504 theropods, and two parallel trackways (TCH1065-T26, TCH1065-T27) assigned to *Jurabrontes*
505 have also been documented. In level CRO500 (Fig. S4), 16 sauropod trackways and 57 tridactyl

506 trackways have been documented. One of the tridactyl trackways (CRO500-T43) has been
507 assigned to Morphotype II (Razzolini et al., 2017). Thus, there are in the three cases a large track
508 type (Morphotype II in BEB500 and CRO500, and *Jurabrontes* in TCH1065) and the robust and
509 the gracile morphotypes in the same surface (Fig. S2-S4). Interestingly, no *Megalosauripus* tracks
510 have been documented in any of the three levels. One way to confirm that some of the small
511 tracks were juveniles of the larger ichnospecies would be to find some kind of relationship among
512 them, such as gregarious behaviour (*sensu* Castanera et al., 2014). In BEB500 (Fig. S2),
513 trackways TR1, TR3, TR4, TR5, TR6 and TR8 (Morphotype II) cross several trackways made by
514 small trackmakers, but the orientations are completely different and do not show any kind of
515 relationship. TR2 (Morphotype II) is subparallel with T34 (small track but unknown morphotype)
516 at the beginning of the trackway but shows a significant change in direction, so this does not
517 show any relationship either. Notably, TR7 (Morphotype II) is a long trackway that is subparallel
518 to T120 (robust morphotype). Tracks T120-L10 and T120-R10 tread over tracks TR7-R8 and
519 TR7-L9 but pass afterwards, so although they show some kind of relation there is no clear
520 evidence of gregarious behaviour. In level TCH1065 (Fig. S3), the two parallel trackways
521 (TCH1065-T26, TCH1065-T27) assigned to *Jurabrontes* do not show any evidence of a
522 relationship with the smaller tracks either. Finally, in CRO500 (Fig. S4), T43 (Morphotype II) is
523 slightly subparallel to T42 (small track but unknown morphotype), but there is no clear evidence
524 to suggest that they were walking together. To sum up, generally the orientation of the large
525 trackways does not seem to suggest any sort of relationship, with the possible exception of TR7
526 and T120. This single case might hint at the hypothesis that some tracks of the robust morphotype
527 (BEB500-T120) might represent a juvenile of the producer of the tracks classified as Morphotype
528 II. Nonetheless, BEB500-T120 is the very trackway that shows more morphometric similarities
529 to *Jurabrontes* than to Morphotype II (Fig. 6). In the light of the previous discussion, the
530 differences between the larger and the smaller morphotypes have thus led us to treat them as
531 different ichnotaxa.

532 3) Ichnotaxonomy:

533 As noted by Marty (2008), small to medium-sized tridactyl tracks are generally not very common
534 in the Late Jurassic and Early Cretaceous, and accordingly such tracks have only recently been
535 the focus of ichnotaxonomic descriptions. Lockley, Meyer and Moratalla (2000) suggested that
536 theropod track morphologies are much more variable through time than previously thought.
537 These authors pointed out that “the perception of morphological conservatism and uniformity
538 through time is, in part, a function of lack of study of adequately large samples of well-preserved
539 material (Baird, 1957)”. In this sense, the studied tracks from the Ajoie ichnoassemblages
540 represent a good sample of tridactyl dinosaur tracks in terms of the number of specimens ($n =$
541 93), with a considerable quality of preservation in many of them ($n = 23$ with a preservation
542 grade greater than 2).

543 Although they are not very abundant in other European tracksites, small to medium-sized
544 tridactyl trackways are the most abundant in the Ajoie ichnoassemblages. As mentioned above,
545 the main small to medium-sized tridactyl dinosaur ichnotaxa that have been described from the
546 Late Jurassic of Europe are (Fig. 7) *Grallator* (Fig. 7A) and *Anomoepus* (Fig. 7B) in Spain

547 (Lockley et al., 2008; Piñuela, 2015; Castanera, Piñuela & García-Ramos, 2016); *Carmelopodus*
548 (Fig. 7C) and *Eubrontes* (Fig. 7D) in France (Mazin et al., 2000; Mazin, Hantzpergue & Pouech,
549 2016); *Wildeichnus* isp. (Fig. 7E), cf. *Jialingpus* (Fig. 7F) and *Dineichnus* (Fig. 7G) in Poland
550 (Gierliński, Niedźwiedzki & Nowacki, 2009); *Dineichnus* (Fig. 7H) (Lockley et al., 1998a) and
551 *Therangospodus*-like tracks (Fig. 7I) (Lockley, Meyer & Moratalla, 2000) in Portugal; and
552 *Grallator* in Germany (Fig. 7J) (Diedrich, 2011). In addition, Conti et al. (2005) described
553 medium-sized footprints (Fig. 7K) that “resemble *Therangospodus*” (their type 3) and another
554 morphotype (their type 2, based on three specimens, Fig. 7L) that shares the same functional
555 character with *Carmelopodus*, i.e., the lack of the fourth proximal pad on digit IV.

556 When compared with the type specimens of these ichnotaxa, the new data on the gracile
557 morphotype of CRO500-T10 (Fig. 8N) (see previous sections) allow us to rule out the presence
558 of *Carmelopodus untermannorum* (Fig. 8A) in the Ajoie, as previously discussed. Generally, the
559 gracile morphotype (Fig. 8M-8O) does not fit with key features of the diagnosis of this
560 ichnotaxon (Lockley et al., 1998b), differing in the phalangeal pad formula (2-3-4 rather than 2-
561 3-3), symmetry, different length/width ratio, or the lower divarication. Among other theropod
562 ichnotaxa, the gracile morphotype shows considerable differences with respect to *Wildeichnus*
563 *navesi* (Fig. 8B, Casamiquela, 1964; Valais, 2011) from the Jurassic of Argentina (as well as
564 larger size, a not subequal but lower divarication angle, larger claw marks, an unrounded digital
565 phalangeal pad in digit IV, greater asymmetry, a generally higher length/width ratio); and with
566 respect to *Therangospodus pandemicus* from the Late Jurassic of North America and Asia (Fig.
567 8C, smaller size, presence of clear phalangeal pads, higher mesaxony) (Lockley et al., 1998a;
568 Fanti et al., 2013). The differences with respect to ornithopod ichnotaxa are noteworthy: it differs
569 from *Anomoepus scambus* (Fig. 8D) in being less symmetric, having a metatarsal-phalangeal pad
570 of digit IV not in line with the digit III axis, no hallux marks, higher mesaxony, and no manus
571 prints present (see Olsen & Rainforth, 2003; Piñuela, 2015). It also differs notably with respect to
572 *Dineichnus socialis* (Fig. 8E, higher FL/FW ratio, higher mesaxony, no quadripartite morphology,
573 a different heel pad impression, lower digit divarication; see Lockley et al., 1998a).

574 The features of the gracile morphotype fit better with those of the tracks assigned to the smaller
575 ichnotaxa of the *Grallator-Anchisauripus-Eubrontes* (Fig. 8F-8H) plexus (Olsen, 1980;
576 Demathieu, 1990; Weems, 1992; Olsen, Smith & McDonald, 1998): small to medium-sized,
577 well-defined digital pads, digits II and IV of similar length, digit III being longer and showing
578 high mesaxony, an oval/subrounded “heel” and a low interdigital angle. Although these footprints
579 have mainly been described from Late Triassic and Early-Middle Jurassic deposits, in recent
580 years they have also been described from younger strata including the Late Jurassic of Europe
581 (see Castanera, Piñuela & García-Ramos, 2016 and references therein). Regarding the use of the
582 ichnotaxon *Anchisauripus*, Castanera, Piñuela & García-Ramos (2016) wrote a short review
583 examining how different authors have considered *Grallator* and *Anchisauripus* as synonyms
584 (Lucas et al., 2006; Lockley, 2009; Piñuela, 2015). The main sample of “grallatorid” tracks that
585 has been described from Late Jurassic deposits in Europe comes from Asturias (Spain), and these
586 have been assigned to *Grallator* (Castanera, Piñuela & García-Ramos, 2016). However, the
587 gracile tracks from the Ajoie ichnoassemblages show some differences from those in Asturias,

588 mainly regarding the digit proportions (FL/FW ratio) and mesaxony (Fig. 9). It should be noted
589 that the Asturian sample shows a great variation in mesaxony (that does not correlate with size).
590 Nonetheless, the gracile morphotype also shows great variations in mesaxony although the
591 footprint proportions are less variable. Although Castanera, Piñuela & García-Ramos (2016)
592 stated that mesaxony “should be used with caution in distinguishing between different
593 ichnotaxa”, we consider that the differences in mesaxony between the gracile morphotype and the
594 *Grallator* tracks are great enough to do so. Furthermore, the FL/FW ratio is also considerably
595 higher in the *Grallator* tracks than in the gracile morphotype. Regarding the *Grallator-Eubrontes*
596 plexus, it is interesting to note the oversplitting that has occurred in some theropod ichnotaxa
597 similar to this plexus. For example, Lockley et al. (2013) propose a great reduction in the Jurassic
598 theropod ichnotaxa from Asia, arguing that many of them were subjective junior synonyms of
599 *Grallator* and *Eubrontes*. Nonetheless, the authors retain the ichnotaxon *Jialingpus yuechiensis*
600 (Fig. 8I) from the Late Jurassic-Early Cretaceous of China (Xing et al., 2014). On the basis of
601 digit proportions (FL/FW ratio) and mesaxony, the gracile morphotype falls partially within the
602 range of *Jialingpus* but also within the range of *Kalohipus bretunensis* (Fig. 8J) from the Lower
603 Cretaceous (Berriasian) of Spain (Fuentes Vidarte & Meijide Calvo, 1998; Castanera et al.,
604 2015). According to Xing et al. (2014), the main differences for distinguishing between
605 *Jialingpus* and *Grallator* are the presence of a digit I trace and the large metatarsophalangeal area
606 positioned in line with digit III, which are its main features. These features are absent in the
607 gracile morphotype, so it cannot be assigned to *Jialingpus*. On the other hand, the diagnosis of
608 *Kalohipus bretunensis* (Fuentes Vidarte & Meijide Calvo, 1998) clearly includes features that
609 distinguish it from the gracile morphotype, such as its smaller size or robust digits, and as seen in
610 Fig. 9, the footprint proportions and especially the mesaxony are also slightly different. As seen
611 in the previous section, the morphology is also different from the larger ichnotaxa (*Jurabrontes*
612 *curtedulensis*, Fig. 8K, and *Megalosauripus transjuranicus*, Fig. 8L) described in the formation.

613 To summarize, the gracile morphotype is quite similar to other grallatorid tracks (*Grallator*,
614 *Anchisauripus*, *Kalohipus*, *Jialingpus*), the main differences being the digit proportions and
615 mesaxony. Given the current state of knowledge, it is difficult to interpret how much variation
616 between the aforementioned ichnotaxa is a consequence of variations in preservation, ontogeny
617 or ichnodiversity. Taking into account the whole discussion, and bearing in mind the high
618 variation in both the FL/FW ratio and mesaxony seen in tracks assigned to *Grallator*, we thus
619 tentatively classify the gracile morphotype as cf. *Kalohipus*, as this is the ichnotaxon that is
620 closest to it. Future studies should elucidate the similarities and differences between these
621 grallatorid tracks, as some *Jialingpus* tracks have been described in the Late Jurassic/Early
622 Cretaceous of Europe (Gierliński, Niedźwiedzki & Nowacki, 2009), and analysis of the
623 differences between *Jialingpus* and other grallatorid tracks (including *Kalohipus*) is “pending”
624 (Xing et al., 2014). In this regard it is interesting to note the differences in mesaxony between
625 both *Kalohipus* and *Jialingpus* (low mesaxony) and *Grallator* (high mesaxony), the question
626 being whether mesaxony is a good ichnotaxobase for discriminating between the three ichnotaxa.
627 Also noteworthy are possible influences on preservation related to the composition of the
628 substrates. For example, *Kalohipus bretunensis* and the main grallatorid ichnotaxa (Fig. 8) are

629 preserved in siliciclastic materials whereas the Swiss Jura tracks cf. *Kalohipus* are preserved in
630 carbonates.

631 Regarding the robust morphotype (Fig. 8P-8Q), a crucial question is whether it represents a
632 single ichnotaxon. In this context, it should be noted that as well as the footprint proportions (Fig.
633 6B), the morphology of the tracks with a preservation grade of 2 or more such as those of
634 trackway BEB500-T120 and the tracks from TCH1065 (TCH1065-T21-R1, TCH1065-E124 and
635 TCH1065-E188) varies considerably. Whatever the case, the morphology of this morphotype
636 *sensu lato* is completely different from that of the ichnotaxa mentioned for the gracile type, such
637 as *Carmelopodus untermannorum* (Fig. 8A, size, phalangeal pad formula, digit divarication,
638 well-developed claw marks), *Wildeichnus navesi* (Fig. 8B, size, gracility, symmetry, length/width
639 ratio and mesaxony), *Anomoepus scambus* (Fig. 8D, size, absence of a manus impression,
640 morphology of the metatarsal-phalangeal pad of digit IV) and *Dineichnus socialis* (Fig. 8E, no
641 quadripartite morphology or circular heel pad impression). Obviously, it is also different from all
642 the aforementioned grallatorid ichnotaxa *Grallator-Anchisauripus-Eubrontes*, plus *Jialingpus*,
643 *Kalohipus* (Fig. 8F-J, mainly in the more robust morphology, footprint proportions, mesaxony,
644 heel morphology, divarication) and the larger ichnotaxa (*Jurabrontes curtedulensis*, Fig. 8K, and
645 *Megalosauripus transjuranicus*, Fig. 8L) described in the formation.

646 It is significant that, of all the known ichnotaxa, the one with most similarities to it is
647 *Therangopodus pandemicus* (Fig. 8C, Lockley, Meyer & Moratalla, 2000), although the robust
648 morphotype has higher digit divarication and probably higher mesaxony (unpublished data for
649 this parameter). According to the original diagnosis, this ichnotaxon is a “medium sized,
650 elongate, asymmetric theropod track with coalesced, elongate, oval digital pads, not separated
651 into discrete phalangeal pads. Trackway narrow with little or no rotation of digit III long axis
652 from trackway axis”. The tracks from the Ajoie ichnoassemblages are slightly smaller in size
653 than *Therangospodus pandemicus* (Lockley, Meyer & Moratalla, 2000; Fanti et al., 2013).
654 According to these authors, and based on the original descriptions by Lockley, Meyer &
655 Moratalla (2000), *Therangospodus* is characterized by: “1) oval digital pads not separated into
656 discrete digital pads, 2) no rotation of digit III, 3) narrow trackway, and 4) relatively reduced size
657 (<30 cm in average length)”. Regarding the absence of discrete digital pads, Lockley, Meyer &
658 Moratalla (2000) described in the type ichnospecies of *Therangospodus* the presence of “faint
659 indentations at the margin of the pads” that sometimes reveal the location of the phalangeal pads,
660 suggesting a 2-3-4 phalangeal pad formula. In this context, Razzolini et al. (2017) commented on
661 the similar features of the tracks described as Morphotype II from the Ajoie ichnoassemblages
662 compared to *Therangospodus* and the problems of assigning some of the tracks to this
663 ichnotaxon. Razzolini et al. (2017) also pointed out the difficulties of distinguishing between
664 *Therangospodus* and *Megalosauripus*, as discussed by other authors previously (Gierliński,
665 Niedźwiedzki & Pieńkowski, 2001; Piñuela, 2015), suggesting that some of the diagnostic
666 features might be extramorphological variations. It is notable that *Megalosauripus* and
667 *Therangospodus* generally co-occur in the same sites (Meyer & Lockley, 1997; Lockley, Meyer
668 & Moratalla, 2000; Lockley, Meyer & Santos, 2000; Xing, Harris & Gierliński, 2011; Fanti et al.,
669 2013), which is relevant as the size and preservation could be the main differences between the

670 two ichnotaxa. Interestingly, as we have seen in the previous section, the tracks described here as
671 belonging to the robust morphotype do not co-occur with any *Megalosauripus* tracks, although
672 some of them (BEB500-T120) co-occur with tracks described as Morphotype II. Even though the
673 robust morphotype is reminiscent of *Therangospodus pandemicus*, it is not possible to assign it to
674 this ichnospecies or to any of the described small-medium-sized ichnotaxa. The scarcity of
675 specimens collected, the preservation grade (none of them as high as 2.5-3) and the doubts as to
676 whether it might represent one or two ichnotaxa prevent us from erecting a new ichnotaxon.
677 Taking into account that *Therangospodus pandemicus* is the closest ichnotaxon described, we
678 thus tentatively classify the tracks from level TCH1065 as cf. *Therangospodus* and the tracks
679 from BEB500 as ?*Therangospodus*. *Therangospodus pandemicus* tracks have been preserved in
680 carbonate materials (Lockley, Meyer & Moratalla, 2000) like the Swiss material, so we can rule
681 out the differences between this ichnotaxon and the robust morphotype being a consequence of
682 this factor.

683 Our analysis of the small to medium-sized footprints adds new data to the dinosaur
684 palaeoecology of carbonate platforms. Generally, it has been thought that carbonate tidal flat
685 deposits are dominated by saurischian assemblages (see Fanti et al., 2013; D’Orazi Porchetti et
686 al., 2016). The gracile morphotype (cf. *Kalohipus*) has been related to the grallatorid ichnotaxa,
687 which have generally been associated with theropod dinosaurs (Olsen, Smith & McDonald, 1998;
688 Lockley, 2009; Fuentes Vidarte & Mejjide Calvo, 1998; Xing et al., 2014; Castanera et al., 2015;
689 Castanera, Piñuela & García-Ramos, 2016). Nonetheless, some authors have suggested that some
690 grallatorid footprints might be attributed to ornithopod dinosaurs (Demathieu, 1990). Regarding
691 the robust morphotype, *Therangospodus pandemicus* is also attributed to theropod dinosaurs
692 (Lockley, Meyer & Moratalla, 2000). Determining whether small-medium-sized tridactyl tracks
693 are attributed to theropods or ornithopods can be problematic. Some features (e.g.: manus
694 impressions, generally low FL/FW ratios and mesaxony, clear sharp claw marks, short pace
695 lengths) have been proposed to distinguish between them, clearly suggesting that the tracks were
696 produced by ornithischians/ornithopods (Castanera et al., 2013a, 2013b and references therein).
697 In the case of the Ajoie ichnoassemblages, there is no evidence of manus impressions and we can
698 rule out a manus preservation bias (e.g.: Castanera et al., 2013a) as the tracks were excavated
699 level-by-level. Only trackway BEB500-T120 has a FL/FW ratio and mesaxony that fall within
700 the parameters of certain ornithopod ichnotaxa (Lockley, 2009; Castanera et al., 2013b, Fig. 9).
701 Clear sharp claw marks have been distinguished in both the gracile and the robust morphotype,
702 with the exception again of BEB500-T120. The pace lengths are reasonably long in all the
703 trackways (Fig. S2). With the current data, the best candidates for producing the minute to small-
704 sized tracks of the Ajoie ichnoassemblages are small-medium-sized theropods, for both the
705 gracile and the robust morphotype (with the possible exception of BEB500-T120). The presence
706 of at least two/three small-sized theropods reported in the present paper, plus the large
707 (*Megalosauripus transjuranicus*, Razzolini et al., 2017) and the giant (*Jurabrontes curtedulensis*)
708 theropod tracks, together with sauropod footprints (Marty, 2008; Marty et al., 2010), support
709 previous assumptions that carbonate tidal flat ichnoassemblages are mainly dominated by
710 saurischian (theropod+sauropod) dinosaurs (Fanti et al., 2013; D’Orazi Porchetti et al., 2016).

711 CONCLUSIONS

712 The minute to medium-sized tridactyl dinosaur tracks from the tracksites of Highway A16 in the
713 Jura Mountains (NW Switzerland) represent one of the largest samples from the Late Jurassic
714 worldwide. Analysis of the quality of preservation (preservation grade), the maximum depth, the
715 shape variation along the trackway, and the footprint proportions (FL/FW ratio and mesaxony)
716 opens a new window onto the interpretation of dinosaur track variations. The description and
717 analysis of the material have made it possible to characterize in detail two different morphotypes,
718 one gracile and one robust, that were already identified in the field. The new data allow us to rule
719 out the notion that the two morphotypes represent a morphological continuum of
720 extramorphological variations, or ontogenetic variations on the larger tracks described from the
721 same sites. An ichnotaxonomical comparison with the main minute to medium-sized tridactyl
722 ichnotaxa has not allowed the studied tracks to be assigned to any known ichnotaxon. On the one
723 hand, the gracile morphotype (cf. *Kalohipus*), though similar to some grallatorid ichnotaxa,
724 shows a number of morphometric differences; on the other hand, the robust morphotype (cf.
725 *Therangospodus* and ?*Therangospodus*), though similar to *Therangospodus pandemicus*, also
726 shows some differences with respect to the diagnosis of the type specimen. Further work is
727 needed in order to understand the possible influence of the substrate composition on theropod
728 ichnotaxonomy in general and the aforementioned ichnotaxa in particular. This study also
729 highlights the difficulties of distinguishing between minute and medium-sized tridactyl dinosaur
730 ichnotaxa and the importance of analysing different factors related to preservation and ontogeny
731 before assigning a single track to a concrete ichnotaxon. The new data increase theropod
732 ichnodiversity to 4/5? theropod ichnotaxa in the tidal flats of the Jura and support previous
733 assumptions that carbonate tidal flats were mainly dominated by theropod and sauropod
734 dinosaurs.

735 REFERENCES

- 736 Alcalá L, Mampel L, Royo-Torres R, Cobos A. 2014. On small quadrupedal ornithopod tracks in
737 Jurassic-Cretaceous transition intertidal deposits (El Castellar, Teruel, Spain). *Spanish Journal of*
738 *Palaeontology* 29 (2):83-190.
- 739 Antunes MT, Mateus O. 2003. Dinosaurs of Portugal. *Comptes Rendus Palevol* 2(1): 77-95.
- 740 Baird D. 1957. Triassic reptile footprint faunules from Milford, New Jersey. *Bulletin of The*
741 *Museum of Comparative Zoology* 117:449-520.
- 742 Belvedere M, Mietto P, Ishigaki S. 2010. A Late Jurassic diverse ichnocoenosis from the
743 siliciclastic Iouaridene Formation (Central High Atlas, Morocco). *Geological Quarterly*
744 54(3):367-380.

- 745 Belvedere M, Farlow JO. 2016. A numerical scale for quantifying the quality of preservation of
746 vertebrate tracks. In: Falkingham PL, Marty D, Richter A, eds. *Dinosaur Tracks—The next steps*.
747 Bloomington and Indianapolis: Indiana University Press. 92-99.
- 748 Campos-Soto S, Cobos A, Caus E, Benito MI, Fernández-Labrador L, Suárez-Gonzalez P,
749 Quijada E, Royo-Torres R, Mas R, Alcalá L. 2017. Jurassic Coastal Park: A great diversity of
750 palaeoenvironments for the dinosaurs of the Villar del Arzobispo Formation (Teruel, eastern
751 Spain). *Palaeogeography, Palaeoclimatology, Palaeoecology* 485: 154-177.
- 752 Casamiquela RM. 1964. Estudios icnológicos: problemas y métodos de la icnología con
753 aplicación al estudio de pisadas mesozoicas, Reptilia, Mammalia de la Patagonia. Librart.
- 754 Castanera D, Vila B, Razzolini NL, Falkingham PL, Canudo JI, Manning PL, Galobart À. 2013a.
755 Manus track preservation bias as a key factor for assessing trackmaker identity and
756 quadrupedalism in basal ornithopods. *PLOS ONE* 8(1), e54177.
- 757 Castanera D, Pascual C, Razzolini NL, Vila B, Barco JL, Canudo JI. 2013b. Discriminating
758 between medium-sized tridactyl trackmakers: tracking ornithopod tracks in the base of the
759 Cretaceous (Berriasian, Spain). *PLOS ONE* 8(11) e81830. doi: 10.1371/journal.pone.0081830.
- 760 Castanera D, Colmenar J, Sauqué V, Canudo JI. 2015. Geometric morphometric analysis applied
761 to theropod tracks from the Lower Cretaceous (Berriasian) of Spain. *Palaeontology* 58(1), 183-
762 200.
- 763 Castanera D, Piñuela L, García-Ramos JC. 2016. *Grallator* theropod tracks from the Late
764 Jurassic of Asturias (Spain): ichnotaxonomic implications. *Spanish Journal of Palaeontology*
765 31(2): 283-296.
- 766 Castanera D, Vila B, Razzolini NL, Santos VF, Pascual C, Canudo JI 2014. Sauropod trackways
767 of the Iberian Peninsula: palaeoetological and palaeoenvironmental implications. *Journal of*
768 *Iberian Geology* 40(1): 49-59.
- 769 Clark ND, Ross DA, Booth P. 2005. Dinosaur tracks from the Kilmaluag Formation (Bathonian,
770 Middle Jurassic) of Score Bay, Isle of Skye, Scotland, UK. *Ichnos* 12(2): 93-104.
- 771 Comment G, Ayer J, Becker D. 2011. Deux nouveaux membres lithostratigraphiques de la
772 Formation de Reuchenette (Kimméridgien, Ajoie, Jura suisse)—Nouvelles données géologiques et
773 paléontologiques acquises dans le cadre de la construction de l'autoroute A16 (Transjurane).
774 *Swiss Bulletin for Applied Geology* 16: 3-24.
- 775 Comment G, Lefort A, Koppka J, Hantzpergue P. 2015. Le Kimméridgien d'Ajoie (Jura, Suisse):
776 lithostratigraphie et biostratigraphie de la Formation de Reuchenette. *Revue de Paléobiologie* 34:
777 161-194.
- 778 Conti MA, Morsilli M, Nicosia U, Sacchi E, Savino V, Wagensommer A, Di Maggio L, Gianolla
779 P. 2005. Jurassic dinosaur footprints from southern Italy: footprints as indicators of constraints in
780 paleogeographic interpretation. *Palaios* 20(6): 534-550.

- 781 Demathieu GR.1990. Problems in discrimination of tridactyl dinosaur footprints, exemplified by
782 the Hettangian trackways, the Causses, France. *Ichnos* 1(2): 97-110.
- 783 Diedrich C. 2011. Upper Jurassic tidal flat megatracksites of Germany –coastal dinosaur
784 migration highways between European islands, and a review of the dinosaur footprints.
785 *Palaeobiodiversity and Palaeoenvironments* 91:129-155.
- 786 D’Orazi Porchetti S, Bernardi M, Cinquegraneli A, Santos VF, Marty D, Petti FM, Caetano PS,
787 Wagensommer, A. 2016.A Review of the Dinosaur Track Record from Jurassic and Cretaceous
788 Shallow Marine Carbonate Depositional Environments.In: Falkingham PL, Marty D, Richter A,
789 eds. Dinosaur Tracks—The next steps. Bloomington and Idianapolis: Indiana University Press.
790 380-392.
- 791 Falkingham PL. 2014. Interpreting ecology and behaviour from the vertebrate fossil track record.
792 *Journal of Zoology* 292(4): 222-228.
- 793 Fanti F, Contessi M, Nigarov A, Esenov P. 2013. New data on two large dinosaur tracksites from
794 the Upper Jurassic of Eastern Turkmenistan (Central Asia). *Ichnos* 20:54-71.
- 795 Foster JR, Lockley MG. 2006. The vertebrate ichnological record of the Morrison Formation
796 (Upper Jurassic, north America). *New Mexico Museum of Natural History and Science Bulletin*
797 36: 203-216.
- 798 Fuentes Vidarte C, Mejjide Calvo M.1998. Icnitas de dinosaurios terópodos en el Weald de Soria
799 (España). Nuevo icnogénero *Kalohipus*. *Estudios Geológicos* 54: 147-152.
- 800 Gatesy SM, Middleton KM, Jenkins Jr FA, Shubin NH.1999. Three-dimensional preservation of
801 foot movements in Triassic theropod dinosaurs.*Nature* 399(6732): 141-144.
- 802 Gierliński GD, Niedźwiedzki G, Pieńkowski G. 2001. Gigantic footprint of a theropod dinosaur
803 in the Early Jurassic of Poland. *Acta Palaeontologica Polonica* 46(3): 441-446.
- 804 Gierliński GD, Niedźwiedzki G, Nowacki P.2009. Small theropod and ornithopod footprints in
805 the Late Jurassic of Poland. *Acta Geologica Polonica* 59(2):221-234.
- 806 Gygi RA. 2000. Annotated index of lithostratigraphic units currently used in the Upper Jurassic
807 of Northern Switzerland. *Eclogae Geologicae Helvetiae* 93:125-146.
- 808 Hammer Ø, Harper DAT, Ryan PD. 2001. PAST: paleontological statistics software package for
809 education and data analysis. *Palaeontologia Electronica* 4: 1-9.
- 810 Hornung JJ, Böhme A, Schlüter N, Reich M.2016. In: Falkingham PL, Marty D, Richter A, eds.
811 Dinosaur Tracks—The next steps. Bloomington and Idianapolis: Indiana University Press.202-
812 225.

- 813 Jank M, Wetzel A, Meyer CA. 2006. A calibrated composite section for the Late Jurassic
814 Reuchenette Formation in northwestern Switzerland (?Oxfordian, Kimmeridgian *sensu gallico*,
815 Ajoie-Region). *Eclogae Geologicae Helvetiae* 99: 175-191.
- 816 Kaever M, de Lapparent AF. 1974. Les traces de pas de dinosaures du Jurassique de Barkhausen
817 (Basse Saxe, Allemagne). *Bulletin de la Société Géologique de France* 16:516-525.
- 818 Lallensack JN, Sander PM, Knötschke N, Wings O. 2015. Dinosaur tracks from the Langenberg
819 Quarry (Late Jurassic, Germany) reconstructed with historical photogrammetry: evidence for
820 large theropods soon after insular dwarfism. *Palaeontologia Electronica* 18.2.31A: 1-34
- 821 Lallensack JN, van Heteren AH, Wings O. 2016. Geometric morphometric analysis of
822 intratrackway variability: a case study on theropod and ornithopod dinosaur trackways from
823 MÜNCHENHAGEN (Lower Cretaceous, Germany). *PeerJ* 4, e2059.
- 824 Lange-Badré B, Dutrieux M, Feyt J, Maury G. 1996. Découverte d'empreintes de pas de
825 dinosaures dans le Jurassique supérieur des Causses du Quercy (Lot, France). *Comptes rendus de*
826 *l'Académie des sciences. Série 2. Sciences de la terre et des planets* 323(1): 89-96.
- 827 Lockley MG. 1994. Dinosaur ontogeny and population structure: interpretations and speculations
828 based on fossil footprints. In: Carpenter K, Hirsch KF, Horner JR, eds. *Dinosaur eggs and babies*.
829 Cambridge University Press. 347-365.
- 830 Lockley MG. 2009. New perspectives on morphological variation in tridactyl footprints: clues to
831 widespread convergence in developmental dynamics. *Geological Quarterly* 53:415-432.
- 832 Lockley MG, Santos VF, Meyer C, Hunt A. 1998a. A new dinosaur tracksite in the Morrison
833 Formation, Boundary Butte, Southeastern Utah. *Modern Geology* 23: 317-330.
- 834 Lockley M, Hunt A, Paquette M, Bilbey SA, Hamblin A. 1998b. Dinosaur tracks from the Carmel
835 Formation, northeastern Utah: implications for Middle Jurassic paleoecology. *Ichnos* 5(4): 255-
836 267.
- 837 Lockley MG, Meyer CA, Moratalla JJ. 2000a. *Therangospodus*: trackway evidence for the
838 widespread distribution of a Late Jurassic theropod with well-padded feet. *Gaia* 15:339-353.
- 839 Lockley MG, Meyer CA, Santos VF. 2000b. *Megalosauripus* and the problematic concept of
840 megalosaur footprints. *Gaia* 15:313-337.
- 841 Lockley M, Mitchell L, Odier GP. 2007. Small theropod track assemblages from Middle Jurassic
842 eolianites of Eastern Utah: paleoecological insights from dune ichnofacies in a transgressive
843 sequence. *Ichnos* 14(1-2): 131-142.
- 844 Lockley MG, Garcia-Ramos JC, Piñuela L, Avanzini M. 2008. A review of vertebrate track
845 assemblages from the Late Jurassic of Asturias, Spain with comparative notes on coeval
846 ichnofaunas from the western USA: implications for faunal diversity in siliciclastic facies
847 assemblages. *Oryctos* 8:53-70.

- 848 Lockley MG, Li JJ, Li RH, Matsukawa M, Harris JD, Xing LD. 2013. A review of the tetrapod
849 track record in China, with special reference to type ichnospecies: implications for
850 ichnotaxonomy and paleobiology. *Acta Geologica Sinica* (English Edition) 87: 1-
- 851 Lucas SG, Klein H, Lockley MG, Spielmann JA, Gierliński GD, Hunt AP, Tanner LH. 2006.
852 Triassic-Jurassic stratigraphic distribution of the theropod footprint ichnogenus *Eubrontes*. *New*
853 *Mexico Museum of Natural History and Science Bulletin* 37: 86-93.
- 854 Mallison H, Wings O. 2014. Photogrammetry in paleontology—A practical guide. *Journal of*
855 *Paleontological Techniques* 12: 1-31.
- 856 Marty D. 2008. Sedimentology, taphonomy, and ichnology of Late Jurassic dinosaur tracks from
857 the Jura carbonate platform (Chevenez– Combe Ronde tracksite, NW Switzerland): insights into
858 the tidal flat palaeoenvironment and dinosaur diversity, locomotion, and palaeoecology.
859 *GeoFocus* 21:1-278.
- 860 Marty D, Meyer CA. 2012. From sauropods to cycads – The Late Jurassic terrestrial record of the
861 Swiss Jura Mountains. In: Witzmann F, Aberhan M, eds. Centen Meet Palaontologische
862 Gesellschaft – Program Abstr F Guid Terra Nostra – Schriften der GeoUnion Alfred-Wegener-
863 Stiftung, Potsdam; 119-120.
- 864 Marty D, Hug W, Iberg A, Cavin L, Meyer C, Lockley M. 2003. Preliminary Report on the
865 Courtedoux Dinosaur Tracksite from the Kimmeridgian of Switzerland. *Ichnos* 10: 209-219.
- 866 Marty D, Cavin L, Hug WA, Jordan P, Lockley MG, Meyer CA. 2004. The protection,
867 conservation and sustainable use of the Courtedoux dinosaur tracksite, Canton Jura, Switzerland.
868 *Rev Paléobiologie* 9:39-49.
- 869 Marty D, Ayer J, Becker D, Berger JP, Billon-Bruyat JP, Braillard L, Hug WA, Meyer CA. 2007.
870 Late Jurassic dinosaur tracksites of the Transjurane highway (Canton Jura, NW Switzerland):
871 overview and measures for their protection and valorisation. *Bulletin für Angewandte Geologie*
872 12: 75-89
- 873 Marty D, Strasser A, Meyer CA. 2009. Formation and taphonomy of human footprints in
874 microbial mats of present-day tidal-flat environments: implications for the study of fossil
875 footprints. *Ichnos* 16(1-2):127-142.
- 876 Marty D, Belvedere M, Meyer CA, Mietto P, Paratte G, Lovis C, Thüning B. 2010. Comparative
877 analysis of Late Jurassic sauropod trackways from the Jura Mountains (NW Switzerland) and the
878 central High Atlas Mountains (Morocco): implications for sauropod ichnotaxonomy. *Historical*
879 *Biology* 22: 109-133.
- 880 Marty D, Meyer CA, Belvedere M, Ayer J, Schafer KL. 2013. Rochefort-Les Grattes: an early
881 Tithonian dinosaur tracksite from the Canton Neuchâtel, Switzerland. *Revue de Paléobiologie*
882 32:373-384.

- 883 Marty D, Belvedere M, Razzolini NL, Paratte G, Cattin M, Lovis C, Meyer C. 2017. The tracks
884 of giant theropods (*Jurabrontes curtedulensis* ichnogen. & ichnosp. nov.) from the Late Jurassic
885 of NW Switzerland: palaeoecological and palaeogeographical implications. *Historical Biology* 1-
886 29.
- 887 Matsukawa M, Lockley MG, Hunt AP. 1999. Three age groups of ornithopods inferred from
888 footprints in the mid-Cretaceous Dakota Group, eastern Colorado, North
889 America. *Palaeogeography, Palaeoclimatology, Palaeoecology* 147(1): 39-51.
- 890 Matthews N, Noble T, Breithaupt B. 2016. Close-Range Photogrammetry for 3-D Ichnology: The
891 Basics of Photogrammetric Ichnology. In: Falkingham PL, Marty D, Richter A, eds. *Dinosaur*
892 *Tracks—The next steps*. Bloomington and Indianapolis: Indiana University Press. 28-55.
- 893 Mazin JM, Hantzpergue P, Bassoullet JP, Lafaurie G, Vignaud P. 1997. The Crayssac site (Lower
894 Tithonian, Quercy, Lot, France): discovery of dinosaur trackways in situ and first ichnological
895 results. *Comptes Rendus de l'Academie des Sciences. Series IIA Earth and Planetary Science*
896 9(325): 733-739.
- 897 Mazin JM, Billon-Bruyat JP, Hantzpergue P, Lafaurie G. 2000. Domination reptilienne dans
898 l'écosystème littoral de Crayssac (Tithonien inférieur, Quercy, Lot). *Bulletin de la Société*
899 *herpétologique de France* 96: 71-81.
- 900 Mazin JM, Hantzpergue P, Pouech J. 2016. The dinosaur tracksite of Loulle (early
901 Kimmeridgian; Jura, France). *Geobios* 49:211-228.
- 902 Meyer CA. 1990. Sauropod tracks from the Upper Jurassic Reuchenette Formation
903 (Kimmeridgian; Lommiswil, Kt. Solothurn) of Northern Switzerland. *Eclogae Geologicae*
904 *Helveticae* 83:389-397.
- 905 Meyer CA, Lockley MG. 1997. Jurassic and Cretaceous dinosaur tracksites from Central Asia
906 (Uzbekistan and Turkmenistan). In: Yang, SY, Huh M, Lee YN, Lockley MG, eds.
907 *Paleontological Society of Korea, Special Publication 2*: 77-92.
- 908 Meyer CA, Thuring B. 2003. Dinosaurs of Switzerland. *Comptes Rendus –Palevol.* 2:103-117.
- 909 Milàn J, Bromley RG. 2006. True tracks, undertracks and eroded tracks, experimental work with
910 tetrapod tracks in laboratory and field. *Palaeogeography, Palaeoclimatology, Palaeoecology*
911 231(3): 253-264.
- 912 Moreau JD, Gand G, Fara E, Michelin A. 2012. Biometric and morphometric approaches on
913 Lower Hettangian dinosaur footprints from the Rodez Strait (Aveyron, France). *Comptes Rendus*
914 *Palevol* 11(4): 231-239.
- 915 Moreau JD, Néraudeau D, Vullo R, Abit D, Mennecart B, Schnyder J. 2017. Late Jurassic
916 dinosaur footprints from Chassiron–La Morelière (Oléron Island, western
917 France). *Palaeobiodiversity and Palaeoenvironments* 97(4):773–789.

- 918 Olsen PE. 1980. Fossil Great Lakes of the Newark Supergroup in New Jersey. In: Manspeizer W.
919 ed. Field Studies of New Jersey Geology and Guide to Field Trips 52nd Annual Meeting New
920 York State Geology Association, Newark College of Arts and Sciences, Newark, Rutgers
921 University, 352-398.
- 922 Olsen PE, Rainforth EC. 2003. The Early Jurassic ornithischian dinosaurian ichnogenus
923 *Anomoepus*. In: LeTourneau PM, Olsen PE, eds. The Great Rift Valleys of Pangea in Eastern
924 North America, Volume 2: Sedimentology, Stratigraphy, and Paleontology, Columbia University
925 Press, 314-367.
- 926 Olsen PE, Smith JB, McDonald NG. 1998. Type material of the type species of the classic
927 theropod footprint genera *Eubrontes*, *Anchisauripus*, and *Grallator* (Early Jurassic, Hartford and
928 Deerfield basins, Connecticut and Massachusetts, USA). *Journal of Vertebrate Paleontology* 18:
929 586-601.
- 930 Pascual-Arribas C, Hernández-Medrano N. 2011. Posibles huellas de crías de terópodo en el
931 yacimiento de Valdehijuelos (Soria, España). *Studia Geologica Salmanticensia* 47 (1): 77-110.
- 932 Piñuela L. 2015. *Huellas de dinosaurios y de otros reptiles del Jurásico Superior de Asturias*. D.
933 Phil. Thesis, Oviedo University.
- 934 Razzolini NL, Vila B, Castanera D, Falkingham PL, Barco JL, Canudo JI, Manning PL, Galobart
935 À. (2014). Intra-trackway morphological variations due to substrate consistency: The El Frontal
936 dinosaur tracksite (Lower Cretaceous, Spain). *PLOS ONE* 9(4), e93708.
- 937 Razzolini NL, Belvedere M, Marty D, Paratte G, Lovis C, Cattin M, Meyer CA. 2017.
938 *Megalosauripus transjuranicus* ichnosp. nov. A new Late Jurassic theropod ichnotaxon from NW
939 Switzerland and implications for tridactyl dinosaur ichnology and ichnotaxomy. *PLOS ONE*
940 12(7): e0180289
- 941 Santisteban C, Gaete R, Galobart A, Suñer M. 2003. Rastros de dinosaurios en el Jurásico
942 terminal (Facies Purbeck) de Corcolilla (Los Serranos, Valencia). In: Pérez Lorente F, Romero
943 Molina MM, Rivas Carrera, P, eds. Dinosaurios y otros reptiles mesozoicos en España. 33-40.
- 944 Santos VF. 2008. *Pegadas de dinossáurios de Portugal*. Museu Nacional de História Natural da
945 Universidade de Lisboa, Lisboa, 123 pp.
- 946 Schudack U, Schudack M, Marty D, Comment G. 2013. Kimmeridgian (Late Jurassic) ostracods
947 from Highway A16 (NW Switzerland): taxonomy, stratigraphy, palaeoecology, and
948 palaeobiogeography. *Swiss Journal of Geosciences* 106: 371-395.
- 949 Schulp AS, Al-Wosabi M. 2012. Telling apart ornithopod and theropod trackways: a closer look at
950 a large, Late Jurassic tridactyl dinosaur trackway at Serwah, Republic of Yemen. *Ichnos* 19(4):
951 194-198.

- 952 Stampfli G, Borel G. 2002. A plate tectonic model for the Paleozoic and Mesozoic constrained by
953 dynamic plate boundaries and restored synthetic oceanic isochrons. *Earth and Planetary Science*
954 *Letters* 196: 17-33.
- 955 Thierry J. 2000. Early Kimmeridgian. In: Dercourt J, Gaetani M, Vrielynck B, Barrier E, Biju-
956 Duval B, Brunet MF, Cadet JP, Crasquin S, Sandulescu M, eds. *Atlas Peri-Tethys,*
957 *Palaeogeographical maps—Explanatory Notes.* CCGM/CGMN (Commission for the Geological
958 *Map of the World*), Paris: 85-97.
- 959 Thierry J, Barrier E, Abbate E, Alekseev AS, Ait-Salem H, Bouaziz S, et al. Map 10: Early
960 Kimmeridgian (146–144 Ma). 2000. In: Dercourt J, Gaetani M, Vrielynck B, Barrier E, Biju-
961 Duval B, Brunet M, et al., editors. *Atlas Peri-Tethys Palaeogeographical maps.* CCGM/CGMN
962 (Commission for the Geological Map of the World), Paris.
- 963 Thulborn T. 1990. *Dinosaur tracks.* Chapman and Hall, London.
- 964 Valais SD. 2011. Revision of dinosaur ichnotaxa from the La Matilde Formation (Middle
965 Jurassic), Santa Cruz Province, Argentina. *Ameghiniana* 48(1): 28-42.
- 966 Waite R, Marty D, Strasser A, Wetzel A. 2013. The lost paleosols: Masked evidence for
967 emergence and soil formation on the Kimmeridgian Jura platform (NW Switzerland).
968 *Palaeogeography, Palaeoclimatology, Palaeoecology* 376: 73-90.
- 969 Weems RE. 1992. A re-evaluation of the taxonomy of Newark Supergroup saurischian dinosaur
970 tracks, using extensive statistical data from a recently exposed tracksite near Culpeper, Virginia.
971 In: Sweet PC, editor. *Proceedings of the 26th forum on the geology of industrial minerals,* 119:
972 113-127.
- 973 Xing LD, Harris JD, Gierliński G. 2011. *Therangospodus* and *Megalosauripus* track assemblage
974 from the Upper Jurassic–Lower Cretaceous Tuchengzi Formation of Chicheng County, Hebei
975 Province, China and their paleoecological implications. *Vertebrata Palasiatica* 49(4): 423-434.
- 976 Xing LD, Lockley MG, Klein H, Gierliński GD, Divay JD, Hu SM, Zhang JP, Ye Y, He YP. 2014.
977 The non-avian theropod track *Jialingpus* from the Cretaceous of the Ordos Basin, China, with a
978 revision of the type material: implications for ichnotaxonomy and trackmaker morphology.
979 *Palaeoworld* 23:187-199.
- 980 Xing LD, Lockley MG, Hu N, Li G, Tong G, Matsukawa M, Klein H, Ye Y, Zhang J, Persons
981 WS. 2016. Saurischian track assemblages from the Lower Cretaceous Shenhuangshan Formation
982 in the Yuanma Basin, Southern China. *Cretaceous Research* 65: 1-9.

983 FIGURE CAPTIONS:

- 984 Fig.1: Geographical and geological settings of the Highway 16 tracksites (modified from
985 Razzolini et al., 2017; Marty et al., 2017). A) Geographical setting of the Ajoie district (NW

986 Switzerland) with the location of the tracksites (1- Courtedoux—Béchat Bovais, 2- Courtedoux—
987 Bois de Sylleux, 3- Courtedoux—Tchâfouè, 4- Courtedoux—Sur Combe Ronde, 5- Chevenez—
988 Combe Ronde, 6- Chevenez—La Combe) along Highway A16. B) Chrono-, bio- and
989 lithostratigraphic setting of the Reuchenette Formation in the Ajoie district, Canton Jura, NW
990 Switzerland (after Comment, Ayer & Becker, 2011, 2015).

991 Fig. 2: Pictures and false-colour depth maps of the tracks with a high preservation grade that
992 belong to the gracile morphotype. A) BEB500-T16-R3; B) BEB500-T26-R5; C) BEB500-T73-
993 L5; D) BSY1020-E2; E) CHV1000-E4; F) CRO500-T10-L10; G) SCR1055-T2-L2*; H)
994 SCR1055-T3-L2*; I) TCH1055-E53; J) TCH1055-T2-L1; K) TCH1060-E58; L) TCH1065-E3;
995 M) TCH1065-E177; N) TCH1065-T25-L2; O) TCH1069-T1-R2. *In these two cases, it is not a
996 picture but a coloured mesh obtained from the 3D-model.

997 Fig. 3: Pictures and false-colour depth maps of the tracks with a high preservation grade that
998 belong to the robust morphotype. A) BEB500-T120-R5; B) BEB500-T120-R6; C) TCH1065-
999 T21-R1; D) TCH1065-E188; E) TCH1065-E124; TCH1065-T15-R1.

1000 Fig. 4: Morphological variation in the footprint shape along the studied trackways from BEB500
1001 tracksite. A) BEB500-T16 (gracile morphotype); B) BEB500-T17 (gracile morphotype); C)
1002 BEB500-T58 (gracile morphotype); D) BEB500-T73 (gracile morphotype); E) BEB500-T75
1003 (gracile morphotype); F) BEB500-T78 (gracile morphotype); G) BEB500-T82 (gracile
1004 morphotype); H) BEB500-T120 (robust morphotype). I) BEB500-T93;

1005 Fig.5: Morphological variation in the footprint shape along the studied trackways from the
1006 CRO500, TCH1055, TCH1065 and TCH1069 tracksites. A) CRO500-T10 (gracile morphotype);
1007 B) CRO500-T30BIS (gracile morphotype); C) TCH1055-T2 (gracile morphotype); D) TCH1065-
1008 T15 (robust morphotype); E) TCH1069-T2 (robust morphotype); F) TCH1065-T25 (gracile
1009 morphotype).

1010 Fig. 6: Bivariate graph plotting the footprint length/footprint width ratio against the mesaxony
1011 (AT) of the studied tracks (gracile and robust morphotype) with the larger tracks described in the
1012 Reuchenette Formation. A) Gracile and robust morphotype compared with *Megalosauripus* tracks
1013 (including tracks classified as *Megalosauripus transjuranicus*, *Megalosauripus cf. transjuranicus*
1014 and *Megalosauripus* isp.), the Morphotype II tracks and *Jurabrontes curtedulensis* (after
1015 Razzolini et al., 2017; Marty et al., 2017). Note that in many cases the points represent tracks
1016 from the same trackway, so variation through the trackway is also represented. B) The studied
1017 tracks compared with just the holotype and paratype specimens of *Megalosauripus*
1018 *transjuranicus* and *Jurabrontes curtedulensis*, plus the best-preserved tracks of Morphotype II
1019 (BEB500-TR7). Outline drawings not to scale.

1020 Fig. 7: Main small-medium-sized tridactyl dinosaur footprints described in the Late Jurassic of
1021 Europe. A) *Grallator* from Spain (S, after Castanera, Piñuela & García-Ramos, 2016); B)
1022 *Anomoepus* from Spain (S, after Piñuela, 2015); C) *Carmelopodus* from France (C, after Mazin,
1023 Hantzpergue & Pouech, 2016); D) *Eubrontes* from France (C, after Mazin et al., 2000); E)
1024 *Wildeckia* from Poland (C, after Gierliński, Niedźwiedzki & Nowacki, 2009); F) *Jialingpus*

1025 from Poland (C, after Gierliński, Niedźwiedzki & Nowacki, 2009). G) *Dineichnus* from Poland
 1026 (C, after Gierliński, Niedźwiedzki & Nowacki, 2009); H) *Dineichnus* from Portugal (S, Lockley
 1027 et al., 1998a); I) *Therangospodus*-like track from Portugal (S, after Lockley, Meyer & Moratalla,
 1028 2000; J) *Therangospodus*-like track from Italy (C, after Conti et al., 2005). K) *Carmelopodus*-like
 1029 track from Italy (C, after Conti et al., 2005); L) *Grallator* from Germany (S, after Diedrich,
 1030 2011). Scale bar = 1 cm (E), 5 cm (A, F, G), 10 cm (B, C, D, H, I, J, K, L). S and C refer to
 1031 siliciclastic and carbonate substrate, respectively.

1032 Fig. 8.: A) Outline drawing of the holotype of *Carmelopodus untermannorum* (S, redrawn after
 1033 Lockley et al., 1998b); B) Outline drawing of the holotype of *Wildeichnus navesi* (V, redrawn
 1034 after Lockley, Mitchel & Odier, 2007); C) Outline drawing of the topotype of *Therangospodus*
 1035 *pandemicus* (S, after Lockley, Meyer & Moratalla, 2000); D) Outline drawing of of *Anomoepus*
 1036 *scambus* (S, after Olsen & Rainforth, 2003); E) Outline drawing of the holotype of *Dineichnus*
 1037 *socialis* (S, after Lockley et al., 1998a); F) Composite outline drawing of type trackway of
 1038 *Grallator parallelus* (S, redrawn from Olsen, Smith & McDonald, 1998); G) Outline drawing of
 1039 type specimen of *Anchisauripus sillimani* (S, redrawn from Olsen, Smith & McDonald, 1998); H)
 1040 Outline drawing of type specimen of *Eubrontes giganteus* (S, redrawn from Olsen, Smith &
 1041 McDonald, 1998). I) Outline drawing of type specimen of *Jialingpus yuechiensis* (S, redrawn
 1042 from Lockley et al., 2013); J) Outline drawing of type specimen of *Kalohipus bretunensis* (S,
 1043 redrawn from Fuentes Vidarte & Meijide Calvo, 1998). K) Outline drawing of type specimen of
 1044 *Jurabrontes curtedulensis* (redrawn from Marty et al., 2017). L) Outline drawing of type
 1045 specimen of *Megalosauripus transjuranicus* (redrawn from Razzolini et al., 2017). M) Outline
 1046 drawing of specimen BSY1020-E2 (cf. *Kalohipus*). N) Outline drawing of specimen CRO500-
 1047 T10-L10 (cf. *Kalohipus*). O) Outline drawing of specimen TCH-1060-E58 (cf. *Kalohipus*); P)
 1048 Outline drawing of specimen TCH-1065-T21-R1 (cf. *Therangospodus*); Q) Outline drawing of
 1049 specimen BEB500-T120-R5 (?*Therangospodus*). S, C and V refer to siliciclastic, carbonate and
 1050 and volcanoclastic substrate, respectively. Scale bar = 2 cm (B, D), 5 cm (F,G, H, I, J), 10 cm (A,
 1051 C, E, L, M-Q), 50 cm (K).

1052 Fig. 9: Bivariate graph plotting the footprint length/footprint width ratio vs AT of the studied
 1053 tracks (gracile and robust morphotype) with some of the main ichnotaxa mentioned in the text.
 1054 Outline drawings not to scale.

1055 Table 1: Measurements of the specimens with a high preservation grade: footprint length (FL),
 1056 footprint width (FW), footprint length /footprint width ratio (FL/FW), digit length (LI, LII, LIII),
 1057 digit width (WI, WII, WIII), divarication angles (II-III, III-IV), mesaxony (AT, anterior triangle
 1058 ratio).

1059 Supplemental information Table S1: List of the specimens analysed, their quality of preservation
 1060 (preservation grade) and the maximum depth. Those with preservation grade 0-0.5 are not
 1061 included in the figshare file. The tracks where the variation along the trackway has been analysed
 1062 are in red.

1063 Supplemental information Figure S2: Map of the Courtedoux—Béchat Bovais tracksite, level 500
1064 (BEB500). In red (gracile) and blue (robust) the minute to medium-sized tridactyl tracks and in
1065 green, the larger morphotype (Morphotype II).

1066 Supplemental information Figure S3: Map of the Courtedoux—Tchâfouè tracksite, level 1065
1067 (TCH1065). In red (gracile) and blue (robust) the minute to medium-sized tridactyl tracks and in
1068 green, the larger morphotype (*Jurabrontes curtedulensis* see Marty et al., 2017).

1069 Supplemental information Figure S4: Map of the Chevenez—Combe Ronde, level 500
1070 (CRO500). In red (gracile) and blue (robust) the minute to medium-sized tridactyl tracks and in
1071 green, the larger morphotype (Morphotype II).

1072 **Acknowledgements**

1073 We thank all technicians, photographers, geometers, drawers, collection managers, and
1074 preparators of the PALA16 that were involved during the excavation and documentation of the
1075 tracksites and during the set-up and organization of the track collection. We also thank the
1076 scientific staff of the PALA16 and JURASSICA Muséum for various stimulating discussions and
1077 valuable input. The authors also thank Laura Piñuela, Vanda Santos, Ignacio Díaz-Martínez, and
1078 Novella L. Razzolini for fruitful discussion on the topic of this manuscript. Rupert Glasgow
1079 revised the English grammar.

Figure 1

Geographical and geological settings of the Highway 16 tracksites (modified from Razzolini et al., 2017; Marty et al., 2017).

A) Geographical setting of the Ajoie district (NW Switzerland) with the location of the tracksites (1- Courtedoux—Béchat Bovais, 2- Courtedoux—Bois de Sylleux, 3- Courtedoux—Tchâfouè, 4- Courtedoux—Sur Combe Ronde, 5- Chevenez—Combe Ronde, 6- Chevenez—La Combe) along Highway A16. B) Chrono-, bio- and lithostratigraphic setting of the Reuchenette Formation in the Ajoie district, Canton Jura, NW Switzerland (after Comment, Ayer & Becker, 2011, 2015).

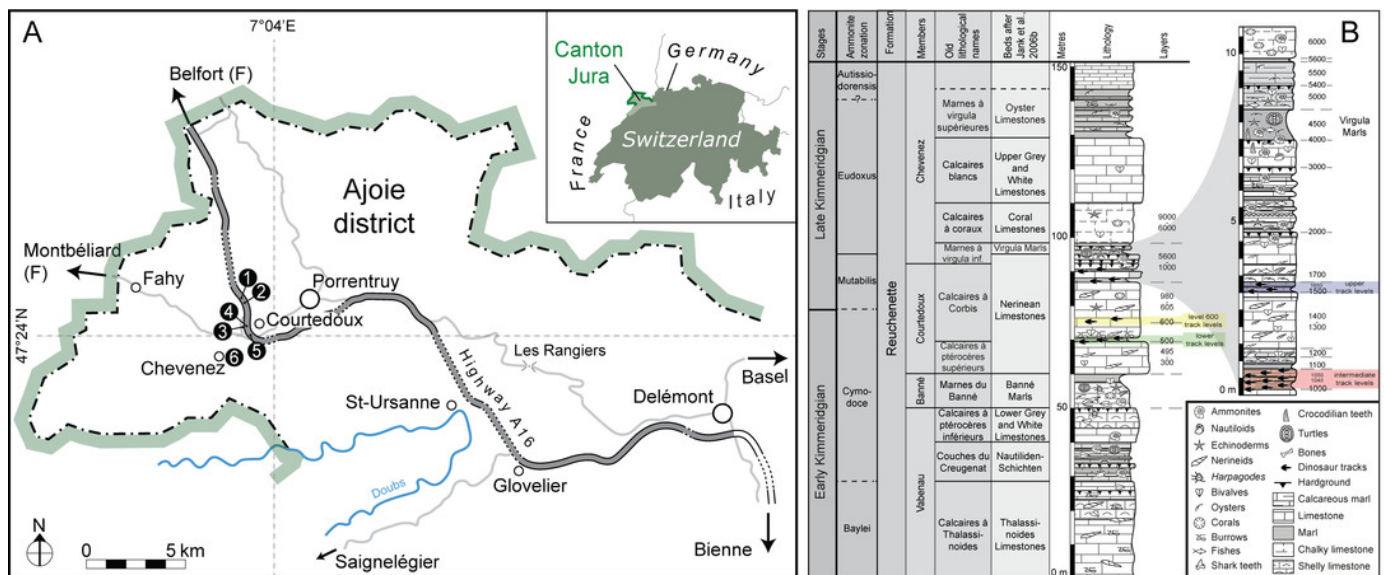


Figure 2

Pictures and false-colour depth maps of the tracks with a high preservation grade that belong to the gracile morphotype.

A) BEB500-T16-R3; B) BEB500-T26-R5; C) BEB500-T73-L5; D) BSY1020-E2; E) CHV1000-E4; F) CRO500-T10-L10; G) SCR1055-T2-L2*; H) SCR1055-T3-L2*; I) TCH1055-E53; J) TCH1055-T2-L1; K) TCH1060-E58; L) TCH1065-E3; M) TCH1065-E177; N) TCH1065-T25-L2; O) TCH1069-T1-R2. *In these two cases, it is not a picture but a coloured mesh obtained from the 3D-model.

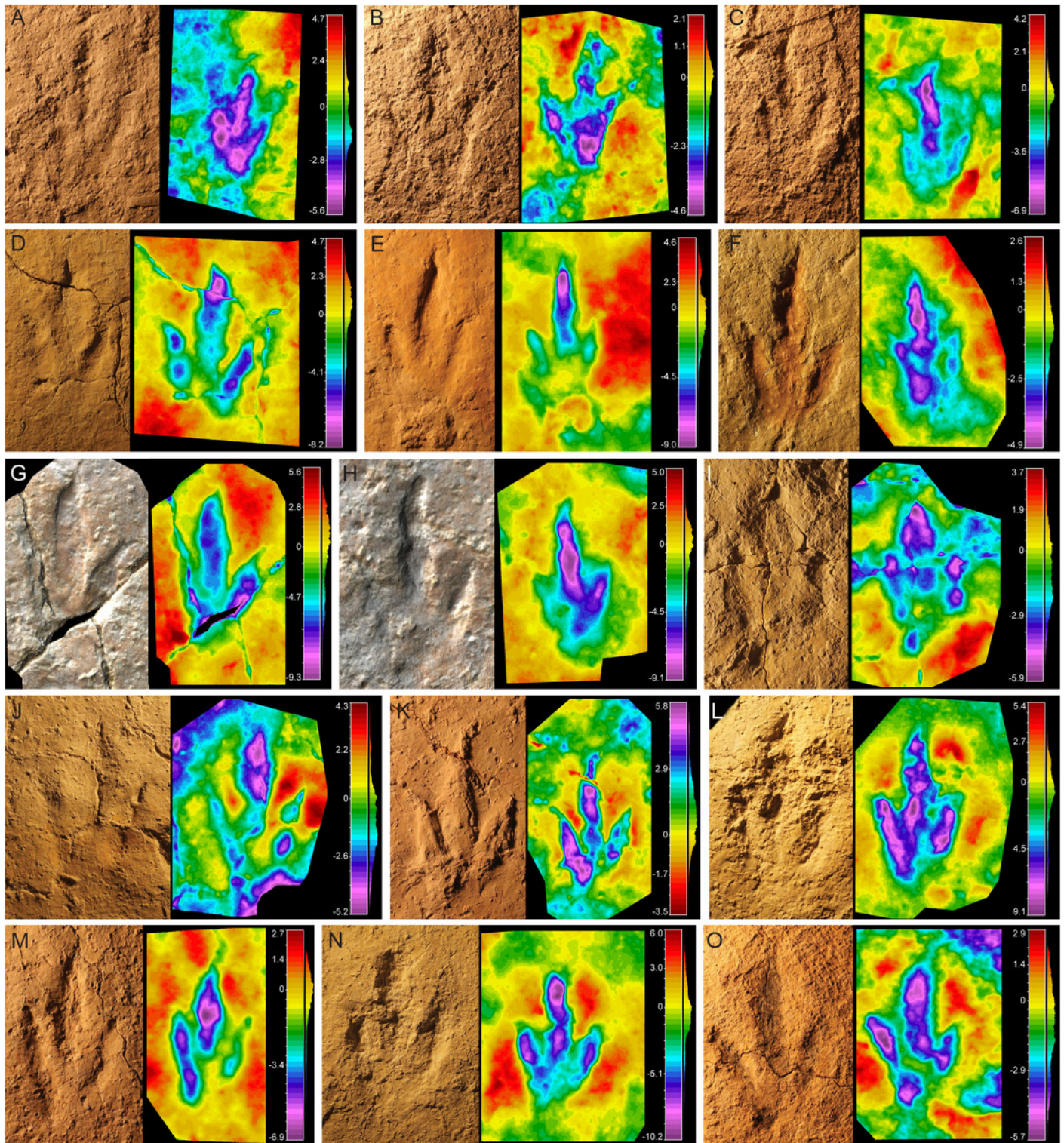


Figure 3

Pictures and false-colour depth maps of the tracks with a high preservation grade that belong to the robust morphotype.

A) BEB500-T120-R5; B) BEB500-T120-R6; C) TCH1065-T21-R1; D) TCH1065-E188; E) TCH1065-E124; TCH1065-T15-R1.

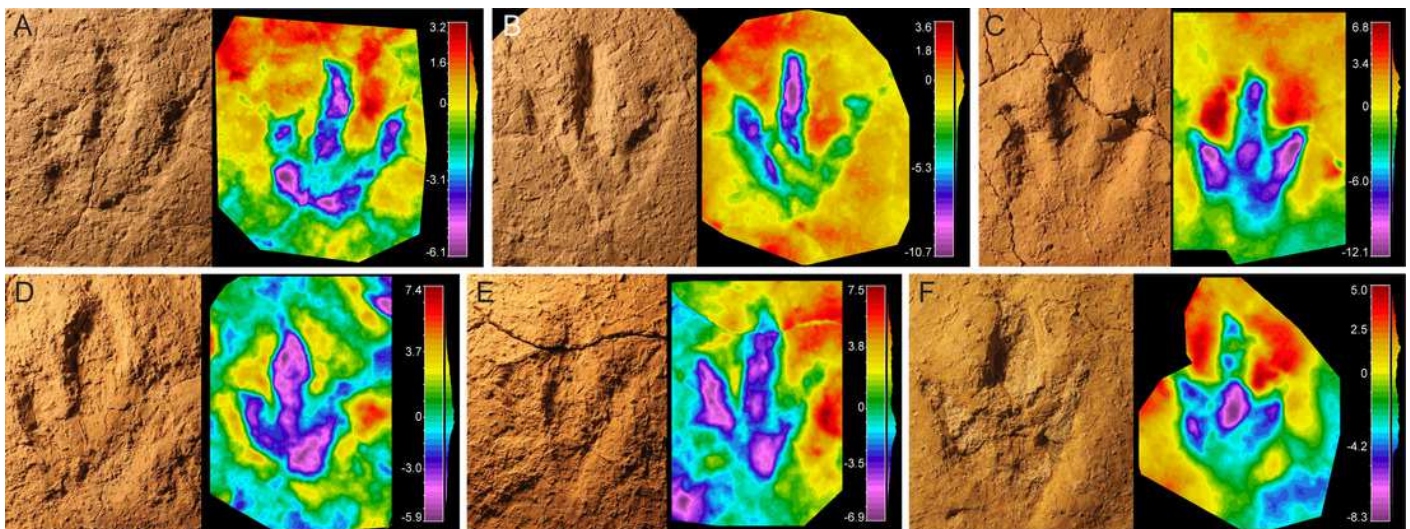


Figure 4

Morphological variation in the footprint shape along the studied trackways from BEB500 tracksite.

A) BEB500-T16 (gracile morphotype); B) BEB500-T17 (gracile morphotype); C) BEB500-T58 (gracile morphotype); D) BEB500-T73 (gracile morphotype); E) BEB500-T75 (gracile morphotype); F) BEB500-T78 (gracile morphotype); G) BEB500-T82 (gracile morphotype); H) BEB500-T120 (robust morphotype). I) BEB500-T93.

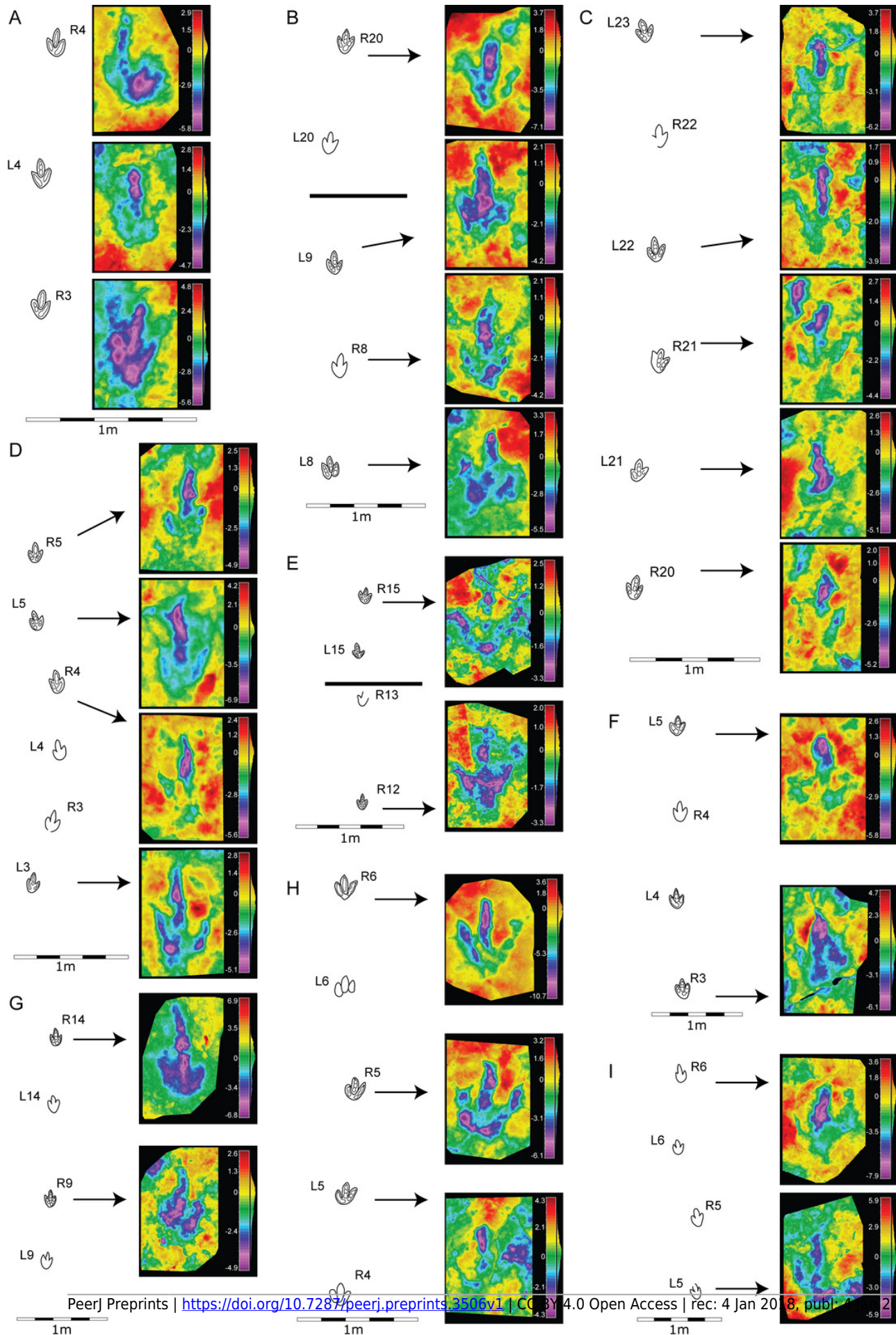


Figure 5

Morphological variation in the footprint shape along the studied trackways from the CRO500, TCH1055, TCH1065 and TCH1069 tracksites.

A) CRO500-T10 (gracile morphotype); B) CRO500-T30BIS (gracile morphotype); C) TCH1055-T2 (gracile morphotype); D) TCH1065-T15 (robust morphotype); E) TCH1069-T2 (robust morphotype); F) TCH1065-T25 (gracile morphotype).

Figure 6

Bivariate graph plotting the footprint length/footprint width ratio against the mesaxony (AT) of the studied tracks (gracile and robust morphotype) with the larger tracks described in the Reuchenette Formation.

A) Gracile and robust morphotype compared with *Megalosauripus* tracks (including tracks classified as *Megalosauripus transjuranicus*, *Megalosauripus cf. transjuranicus* and *Megalosauripus isp.*), the Morphotype II tracks and *Jurabrontes curtedulensis* (after Razzolini et al., 2017; Marty et al., 2017). Note that in many cases the points represent tracks from the same trackway, so variation through the trackway is also represented. B) The studied tracks compared with just the holotype and paratype specimens of *Megalosauripus transjuranicus* and *Jurabrontes curtedulensis*, plus the best-preserved tracks of Morphotype II (BEB500-TR7). Outline drawings not to scale.

Figure 7

Main small-medium-sized tridactyl dinosaur footprints described in the Late Jurassic of Europe.

A) *Grallator* from Spain (S, after Castanera, Piñuela & García-Ramos, 2016); B) *Anomoepus* from Spain (S, after Piñuela, 2015); C) *Carmelopodus* from France (C, after Mazin, Hantzpergue & Pouech, 2016); D) *Eubrontes* from France (C, after Mazin et al., 2000); E) *Wildeichnus* from Poland (C, after Gierliński, Niedźwiedzki & Nowacki, 2009); F) *Jialingpus* from Poland (C, after Gierliński, Niedźwiedzki & Nowacki, 2009). G) *Dineichnus* from Poland (C, after Gierliński, Niedźwiedzki & Nowacki, 2009); H) *Dineichnus* from Portugal (S, Lockley et al., 1998a); I) *Therangospodus*-like track from Portugal (S, after Lockley, Meyer & Moratalla, 2000; J) *Therangospodus*-like track from Italy (C, after Conti et al., 2005). K) *Carmelopodus*-like track from Italy (C, after Conti et al., 2005); L) *Grallator* from Germany (S, after Diedrich, 2011). Scale bar = 1cm (E), 5 cm (A, F, G), 10 cm (B, C, D, H, I, J, K, L). S and C refer to siliciclastic and carbonate substrate, respectively.

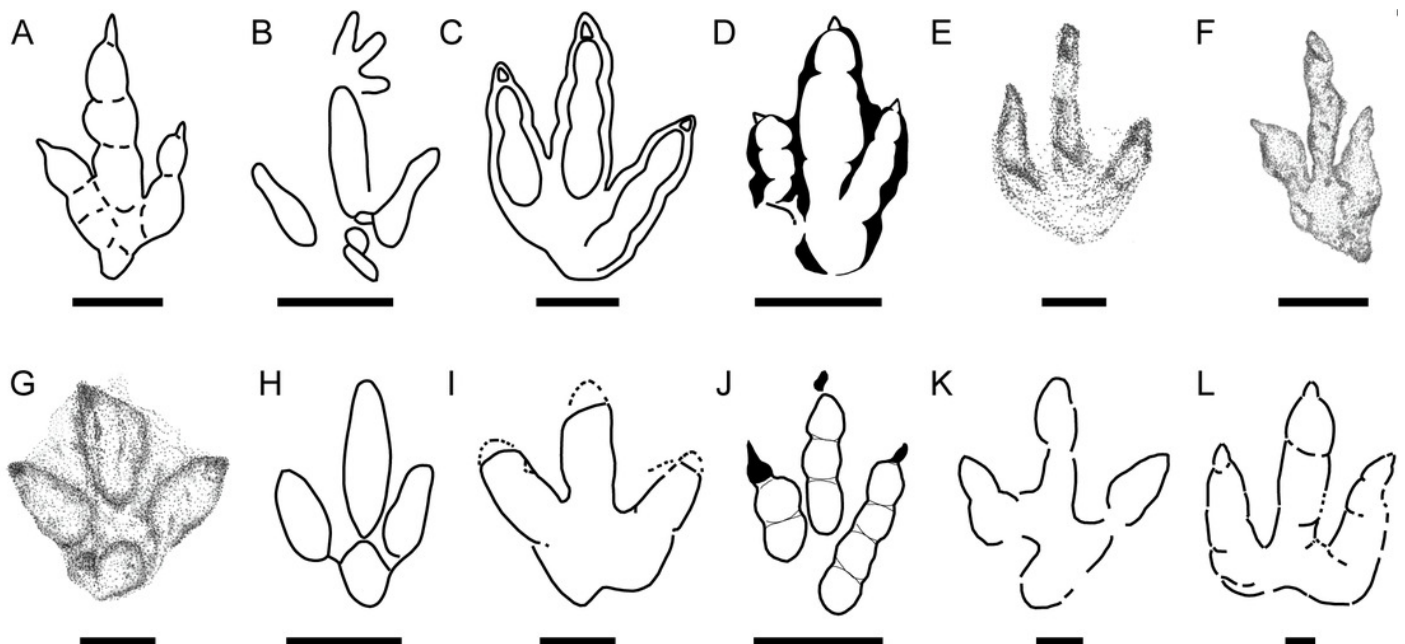


Figure 8

Small-medium-sized tridactyl dinosaur ichnotaxa with affinities with the described morphotypes.

A) Outline drawing of the holotype of *Carmelopodus untermannorum* (S, redrawn after Lockley et al., 1998b); B) Outline drawing of the holotype of *Wildeichnus navesi* (V, redrawn after Lockley, Mitchel & Odier, 2007); C) Outline drawing of the topotype of *Therangospodus pandemicus* (S, after Lockley, Meyer & Moratalla, 2000); D) Outline drawing of of *Anomoepus scambus* (S, after Olsen & Rainforth, 2003); E) Outline drawing of the holotype of *Dineichnus socialis* (S, after Lockley et al., 1998a); F) Composite outline drawing of type trackway of *Grallator parallelus* (S, redrawn from Olsen, Smith & McDonald, 1998); G) Outline drawing of type specimen of *Anchisauripus sillimani* (S, redrawn from Olsen, Smith & McDonald, 1998); H) Outline drawing of type specimen of *Eubrontes giganteus* (S, redrawn from Olsen, Smith & McDonald, 1998). I) Outline drawing of type specimen of *Jialingpus yuechiensis* (S, redrawn from Lockley et al., 2013); J) Outline drawing of type specimen of *Kalohipus bretunensis* (S, redrawn from Fuentes Vidarte & Mejjide Calvo, 1998). K) Outline drawing of type specimen of *Jurabrontes curtedulensis* (redrawn from Marty et al., 2017). L) Outline drawing of type specimen of *Megalosauripus transjuranicus* (redrawn from Razzolini et al., 2017). M) Outline drawing of specimen BSY1020-E2 (cf. *Kalohipus*). N) Outline drawing of specimen CRO500-T10-L10 (cf. *Kalohipus*). O) Outline drawing of specimen TCH-1060-E58 (cf. *Kalohipus*); P) Outline drawing of specimen TCH-1065-T21-R1 (cf. *Therangospodus*); Q) Outline drawing of specimen BEB500-T120-R5 (?*Therangospodus*). S, C and V refer to siliciclastic, carbonate and and volcanoclastic substrate, respectively. Scale bar = 2 cm (B, D), 5 cm (F,G, H, I, J), 10 cm (A, C, E, L, M-Q), 50 cm (K).

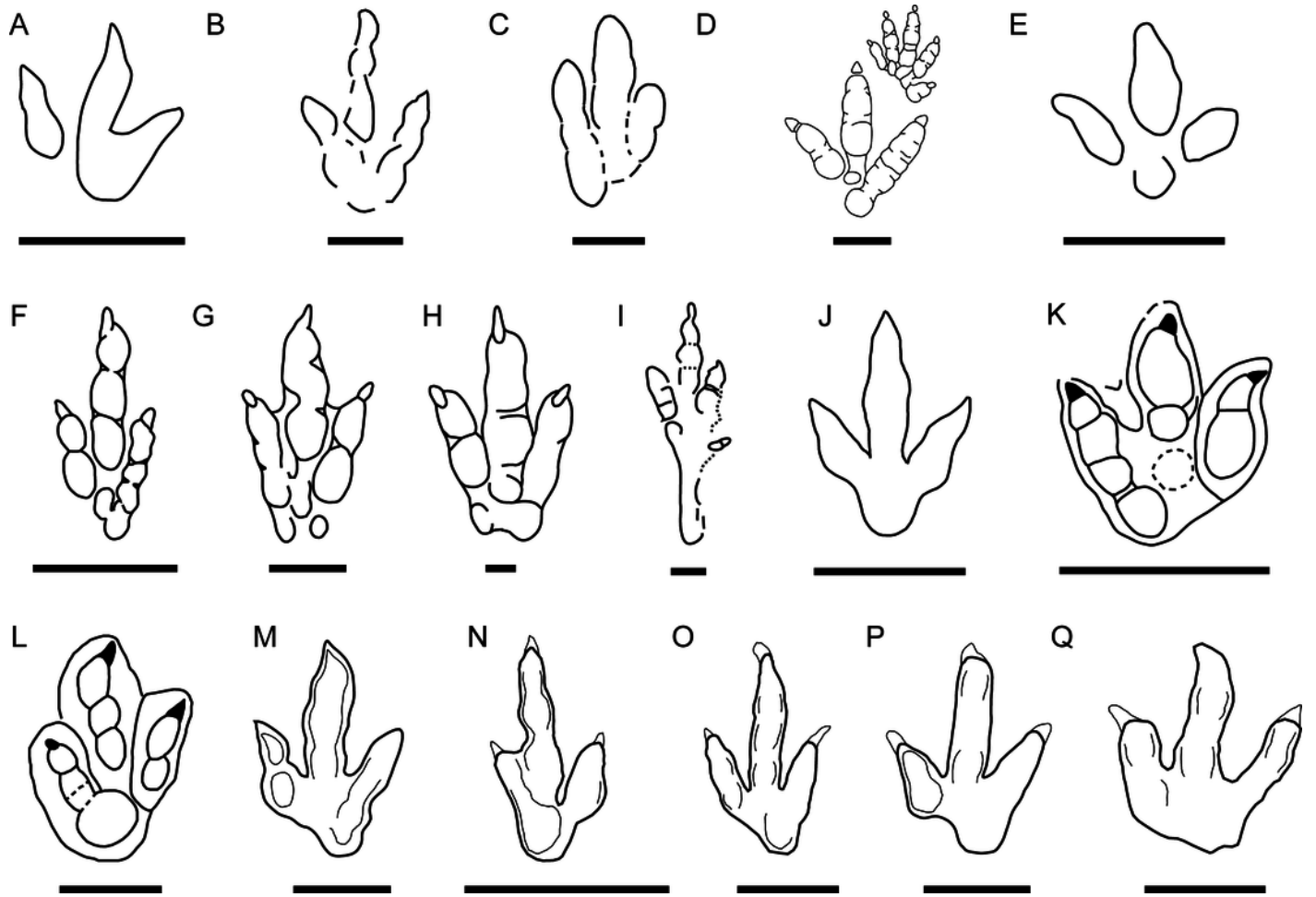


Figure 9

Bivariate graph plotting the footprint length/footprint width ratio against AT of the studied tracks (gracile and robust morphotype) with some of the main ichnotaxa mentioned in the text.

Outline drawings not to scale.

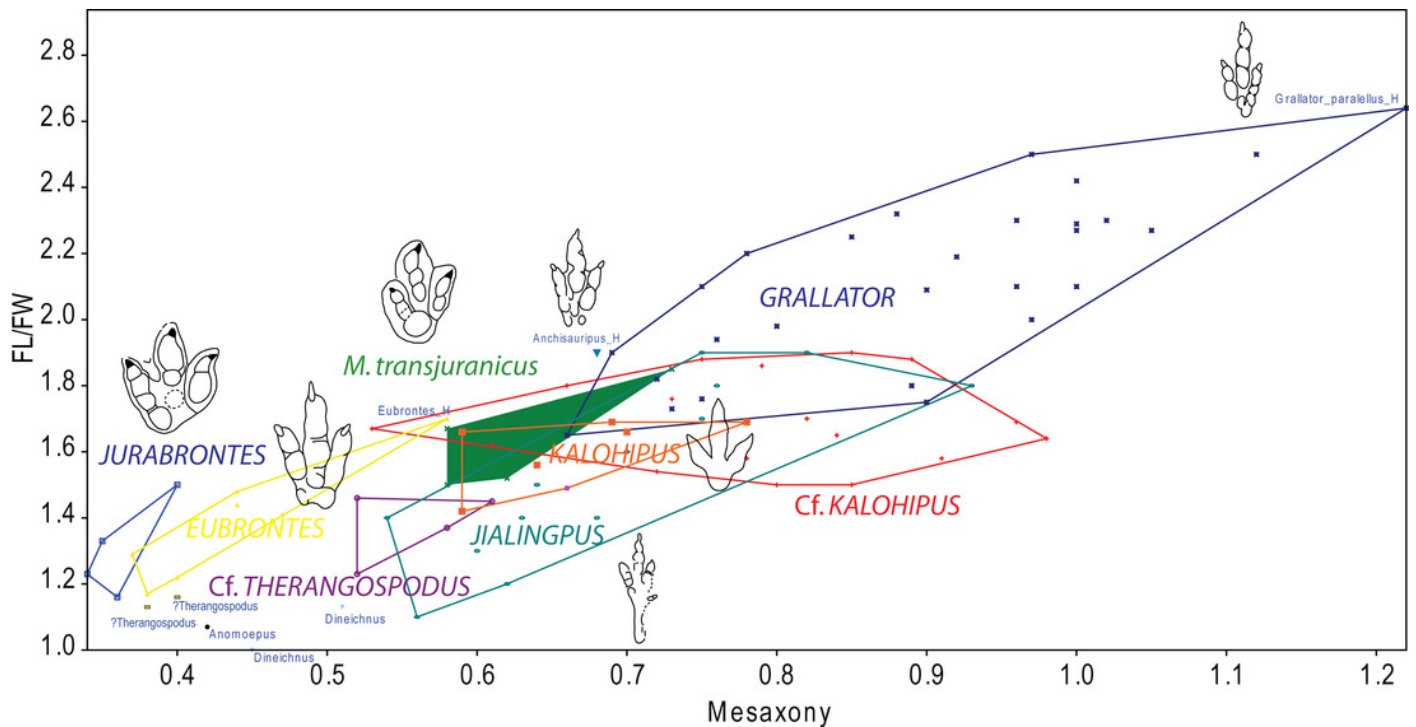


Table 1 (on next page)

Measurements of the specimens with a high preservation grade:

footprint length (FL), footprint width (FW), footprint length /footprint width ratio (FL/FW), digit length (LI, LII, LIII), digit width (WI, WII, WIII), divarication angles (II-III, III-IV), mesaxony (AT, anterior triangle ratio).

Track	FL	FW	FL/FW	LII	LIII	LIV	WII	WIII	WIV	II^III	III^IV	ATw	Atl	AT
BEB500-T16-R3	18	10	1.8	13.5	18	13.8	2	1.9	1.8	22.5	17.5	8.8	5.8	0.66
BEB500-T17-R8	19	11.5	1.65	11	19	13	1.9	3.3	1.6	23	20	10.5	8.8	0.84
BEB500-T26-R5	19	12	1.58	13	19	14	2.2	3	2.9	32	26	10.3	9.4	0.91
BEB500-T73-L5	15	8.5	1.76	8.5	15	10	2.3	2.9	2.5	31	22	7.9	5.8	0.73
BSY1020-E2	22	11.7	1.88	15	22	13.5	3.6	3	2.7	21.5	24.5	9.5	8.5	0.89
TCH1055-E53	17.5	10.3	1.7	12.2	17.5	12	3	2.7	2.5	25	17.5	8.5	7	0.82
TCH1055-T2-L1	21.2	13.1	1.62	15.6	21.2	15	2.3	2.1	2.2	25	22	11.4	7	0.61
TCH1055-T2-R1	19.5	13	1.5	13.2	20.5	13.1	3.3	3.7	2.5	29	23	10.6	8.5	0.80
TCH1060-E58	20	10.5	1.90	20	13.5	12	3.4	3.1	2.9	27	22	8.8	7.5	0.85
TCH1065-E177	17.5	9.4	1.86	11.8	17.5	12.5	1.6	2.4	2	21	20	8.2	6.5	0.79
TCH1065-E3	18.4	12.3	1.5	12.3	18.4	11.7	3.3	3.8	2.3	30	24	9.14	7.8	0.85
TCH1065-T25-L2	19.3	12.2	1.58	14	19.3	12.3	3	3	2.7	25	21	10.3	8	0.78
TCH1069-T1-R2	20	13	1.54	14	20	13.5	2.1	2.7	2.1	24	29	11.5	8.3	0.72
SCR1055-T2-L2	20	12	1.67	15	20	16	2.7	2.9	2.5	25	18	11.4	6	0.53
SCR1055-T3-L2	18	11	1.64	12	18	12	2.3	2.1	1.8	26	26	8.5	8.3	0.98
CHV1000-E4	16	8.5	1.88	11	16	10	1.8	2.3	1.7	21	22	8.1	6.1	0.75
CRO500-T10-L10	11	6.5	1.69	6	11	7	1.4	1.8	1.5	32	23	5.6	5.4	0.96
BEB500-T120-R5	17	15	1.13	13.5	17	14.5	3.5	3.2	2.5	30.4	34	13	5	0.38
BEB500-T120-R6	18	15.5	1.16	14.5	18	15	2.5	3.1	3	22	27	14.2	5.7	0.40
TCH1065-E124	19	15.5	1.23	13.5	19	15	3.3	4.5	3.5	27.5	26.5	14.4	7.5	0.52
TCH1065-E188	18	12.3	1.46	13.3	18	13	3.2	3.7	3.3	25	27	10	5.2	0.52
TCH1065-T21-R1	19.8	14.5	1.37	14.4	19.8	14.8	3.5	3.7	3.5	27	27	11.8	6.9	0.58
TCH1065-T15-R1	21.8	15	1.45	15.7	21.8	17.2	2.7	3.4	3.1	29	25	12	7.3	0.61